NAVAL POSTGRADUATE SCHOOL

MONTEREY, CALIFORNIA

THESIS

DUAL-HARDNESS TITANIUM BODY ARMOR FOR CONCEALABLE APPLICATIONS

by

Berl McLaurin

June 2018

Thesis Advisor:	Raymond M. Gamache
Second Reader:	Emil P. Kartalov

Approved for public release. Distribution is unlimited.

THIS PAGE INTENTIONALLY LEFT BLANK

REPORT DOCUMENTATION PAGE			*Form Approved OMB No. 0704-0188*

1. AGENCY USE ONLY *(Leave blank)*	**2. REPORT DATE** June 2018	**3. REPORT TYPE AND DATES COVERED** Master's thesis

4. TITLE AND SUBTITLE DUAL-HARDNESS TITANIUM BODY ARMOR FOR CONCEALABLE APPLICATIONS	**5. FUNDING NUMBERS** RPLBX
6. AUTHOR(S) Berl McLaurin	
7. PERFORMING ORGANIZATION NAME(S) AND ADDRESS(ES) Naval Postgraduate School Monterey, CA 93943-5000	**8. PERFORMING ORGANIZATION REPORT NUMBER**
9. SPONSORING / MONITORING AGENCY NAME(S) AND ADDRESS(ES) N/A	**10. SPONSORING / MONITORING AGENCY REPORT NUMBER**

11. SUPPLEMENTARY NOTES The views expressed in this thesis are those of the author and do not reflect the official policy or position of the Department of Defense or the U.S. Government.

12a. DISTRIBUTION / AVAILABILITY STATEMENT Approved for public release. Distribution is unlimited.	**12b. DISTRIBUTION CODE** A

13. ABSTRACT (maximum 200 words)

A current need exists to develop a lightweight, low-profile armor system capable of defeating a 7.62x39mm ball round at muzzle velocity. Three design requirements must be met within the development of this system: areal density less than 5lbs/ft^2, an overall thickness of less than 8mm, and formability to match torso contours. This study focuses on pure titanium (Ti) (Grade 2) and a single titanium alloy, Ti6Al-4V (Grade 5). Both materials exhibit superplastic behavior to enable shaping to the torso. Initial studies focus on laminate systems of both homogeneous and heterogeneous layered structures to investigate pressure reduction mechanisms. In addition to layered systems, hard front face coatings are studied as an alternative approach to reducing the penetration pressure through initial blunting of the incident projectile. Test configurations are investigated both experimentally and through hydrocode modeling.

14. SUBJECT TERMS armor, titanium, body, weapons, penetration, superplastic, Ti6Al4V, 7.62x39mm, concealable, thin, lightweight	**15. NUMBER OF PAGES** 87
	16. PRICE CODE

17. SECURITY CLASSIFICATION OF REPORT Unclassified	**18. SECURITY CLASSIFICATION OF THIS PAGE** Unclassified	**19. SECURITY CLASSIFICATION OF ABSTRACT** Unclassified	**20. LIMITATION OF ABSTRACT** UU

NSN 7540-01-280-5500

Standard Form 298 (Rev. 2-89)
Prescribed by ANSI Std. 239-18

THIS PAGE INTENTIONALLY LEFT BLANK

Approved for public release. Distribution is unlimited.

DUAL-HARDNESS TITANIUM BODY ARMOR FOR CONCEALABLE APPLICATIONS

Berl McLaurin
Ensign, United States Navy
BS, United States Naval Academy, 2017

Submitted in partial fulfillment of the
requirements for the degree of

MASTER OF SCIENCE IN PHYSICS

from the

NAVAL POSTGRADUATE SCHOOL
June 2018

Approved by: Raymond M. Gamache
Advisor

Emil P. Kartalov
Second Reader

Kevin B. Smith
Chair, Department of Physics

THIS PAGE INTENTIONALLY LEFT BLANK

ABSTRACT

A current need exists to develop a lightweight, low-profile armor system capable of defeating a 7.62x39mm ball round at muzzle velocity. Three design requirements must be met within the development of this system: areal density less than 5lbs/ft^2, an overall thickness of less than 8mm, and formability to match torso contours. This study focuses on pure titanium (Ti) (Grade 2) and a single titanium alloy, Ti6Al-4V (Grade 5). Both materials exhibit superplastic behavior to enable shaping to the torso. Initial studies focus on laminate systems of both homogeneous and heterogeneous layered structures to investigate pressure reduction mechanisms. In addition to layered systems, hard front face coatings are studied as an alternative approach to reducing the penetration pressure through initial blunting of the incident projectile. Test configurations are investigated both experimentally and through hydrocode modeling.

THIS PAGE INTENTIONALLY LEFT BLANK

TABLE OF CONTENTS

LIST OF FIGURES

LIST OF TABLES

LIST OF ACRONYMS AND ABBREVIATIONS

Al_2O_3	Alumina
AlTiN	Aluminum Titanium Nitride
BN	Boron Nitride
(E)SAPI	(Enhanced) Small Arms Protective Inserts
G2	Titanium Grade 2
HEL	Hugoniot Elastic Limit
IBA	Interceptor multi-threat Body Armor system
PC	Polycarbonate
PVD	Physical Vapor Deposition
Ti	Titanium
SiC	Silicon Carbide
Ti6Al4V or G5	Titanium-6-Aluminum-4-Valadium (Grade 5)
TiB_2	Titanium Diboride
TiN	Titanium Nitride
UHMWPE	Ultra-High Molecular Weight Polyethylene

THIS PAGE INTENTIONALLY LEFT BLANK

ACKNOWLEDGMENTS

Special thanks to the gun range crew at NSWC Dahlgren who were instrumental in getting ballistics tests done.

THIS PAGE INTENTIONALLY LEFT BLANK

I. INTRODUCTION

A. MOTIVATION

The United States conducts operations all around the globe. Many of these operations involve “high-priority” personnel such as diplomats, intelligence agents, and special operators. Individuals working in this capacity may occasionally find themselves in need of protection from small arms fire.

Existing body armor systems are bulky and cumbersome. The most common type of body armor employed by the United States armed forces is the Interceptor Multi-threat Body Armor System (IBA), which consists of a tactical vest and optional groin, throat, and bicep protectors. The IBA has four pockets that enable the placement of four ceramic plates called Small Arms Protective Inserts (SAPIs). The plates can be over 1 inch thick (ESAPI) and can weigh in excess of 7 pounds each. In total, the IBA system with protective plates can add up to 16.4 pounds of weight to the wearer.

These systems are conspicuous. For various reasons, many government actors may not want to draw attention to themselves in the performance of their duties. Wearing a large camouflage bullet-proof vest is not ideal for covert operations.

Current composite armor systems are fragile. Printed prominently on the front of the SAPI plate is the familiar phrase, “HANDLE WITH CARE.” While incredibly hard and effective for stopping bullets, the brittle nature of ceramics makes them highly susceptible to inadvertent damage, rendering them useless to the wearer.

B. OBJECTIVE

The current research aims to create a durable, lightweight, concealable body armor system for use by U.S. government actors in potentially hostile operating areas.

1. Design Constraints

The sponsors have provided specific requirements for the system.

- Maximum areal density of 5 pounds per square foot

- Maximum thickness of 8 millimeters
- Effective against AK-47 7.62x39mm ball round

2. Threat Analysis

The AK-47 fires a 7.62x39mm ball round at a muzzle velocity of approximately 747 meters per second (2450 fps). The projectile is 2.7 centimeters long and has a diameter of 7.9 millimeters, and a mass of 124 grains (8 grams). It comprises a low carbon steel core encased in a copper jacket and lead filler. A cutaway of the projectile is shown in Figure 1. As shown in Figure 1, the core has a flat tip, making it less effective for penetrating hard armors.

Figure 1. Cutaway of 7.62x39mm ball round

C. THESIS ORGANIZATION

This thesis is divided into six chapters. Chapter I introduced the current problem and the objective of this research. Chapter II provides an explanation of the key concepts and realistic evaluation of armors and titanium alloys as they pertain to this investigation. Chapter III details the experimental setup as well as the various approaches with which the problem is addressed. Experimental work was done in parallel with computer modeling, also discussed in Chapter III. Chapter IV is a chronological explanation of each ballistic test series along with the data collected for each case. Chapter V is an analysis of the data tabulated in Chapter IV and includes validation of trends by computational modeling. Finally, Chapter VI provides a succinct summary of the findings, successes, and shortcomings of this research. The feasibility of a concealable titanium body armor is discussed along with further work that is yet to be completed.

As is customary in the field of ballistics, imperial units will be used for some measurements (areal density, mass efficiency, muzzle velocity, etc.) while metric units will be used for others.

THIS PAGE INTENTIONALLY LEFT BLANK

II. BACKGROUND

A. IMPACT DYNAMICS

Impact pressure from a ballistic impact is dependent on multiple factors, including impact velocity material densities and strengths (both projectile and target). Depending on the impact pressure and material behavior, both projectile and target may exhibit fluid-like behavior when the impact pressures exceed the mechanical strength of either, or both, the impactor and target materials.

Tate demonstrated that at high velocities, penetrators impacting hard surfaces behaved as fluids rather than rigid objects [1]. Within every solid material there are measurable strength properties that affect their behavior under these conditions. He found this to be dependent on two quantities: the pressure within the target at which the material begins to flow hydrodynamically, and the pressure at which the penetrating rod begins to flow hydrodynamically. The hydrodynamic behavior is dependent on the impact pressure exceeding the elastic limit and beginning to plasticly deform. Under dynamic conditions, the Hugoniot Elastic Limit (HEL) defines the impact pressure beyond which plastic deformation is initiated [1]. Tate calculated that for targets and penetrators of the same material, the target’s flow pressure is greater than that of the penetrator, and that the assumption of constant velocity during penetration is a valid approximation. This information can serve as a simplistic view of the incorporation of a hard front face applied to an armor system where an initial hard front face can introduce plastic deformation to an incident sharp ogive projectile enabling a decrease in pressure.

B. MEASURING BALLISTIC PERFORMANCE OF ARMOR

The dynamic behavior of ballistic penetration creates variations in damage mechanisms as compared to static conditions. Armor performance must be assessed under dynamic conditions. Testing under dynamic conditions is typically performed using one of two techniques: V-50 or V-0.

V-50 testing is a technique that enables a specific performance level to be measured by a specific round. V-50 is defined as the velocity for a specific projectile where it will penetrate the studied target 50% of the time. V-50 testing can incorporate specific bullets or fragment simulating projectiles. Within a V-50 test the impact velocity of a selected projectile is varied enabling conditions of both complete and partial penetrations. Based on the number of tests, the difference in impact velocity between complete and partial penetrations have an allowed variance between 15 and 30 m/s. V-50 measurements are very important in understanding the specific performance of an armor system for a specific round.

V-0 testing typically involves a specific projectile impacting a target and providing a statistical confidence that target penetration will have a 0% probability. The number of impacts to provide statistical certainty are typically dictated by an end user requirement or governing agency.

As a rule of thumb, V-50 testing is typically performed within the research and development community and V-0 is performed within matured armor technologies in preparation for fielding.

C. ARMOR DESIGN APPROACHES

Within this thesis, the ability to enable the target material to resist penetration is of great importance. Many techniques exist to reduce the penetration pressure of the projectile through purposely designed components. From a fundamental view, the impact pressure can be simply viewed as the force divided by the area of the projectile. In addition, the force can be further viewed as the change in momentum over time.

$$Impact\ Pressure = \frac{Force}{Area} = \frac{\frac{dP}{dt}}{Area} \tag{1}$$

Based on equation 1, we can observe two paths to decrease the penetration pressure of projectile on the armor system. The first technique is to increase the time period within which the projectile momentum is arrested and the second is to increase the surface area of the projectile through blunting or breakup. Both techniques can contribute to a reduction in penetration within an armor system.

Standard techniques to reduce the penetration pressure through impact area amplification include blunting, breaking/shattering and tripping of an incident projectile.

An approach to perform both blunting and projectile breakup is through a hard front surface which exceeds the strength of the incident projectile. During impact either surface area amplification or projectile breakup can occur. Issues exist with this approach as hardened materials lack the ductility to dissipate energy through deformation of the target. The hardened materials tend to generate a higher dP/dt term and will cause unwanted failures through sheer plugging or shattering of the target front face.

Techniques to increase the arresting time of a projectile can greatly reduce the forces during projectile deceleration. Key materials include mild steel and textiles that enable deformation and flexure. Issues with this approach include the inability to deform projectiles and susceptibility to premature perforation from sharp ogive projectiles.

Current high-performance armor includes a hard front face material backed by a compliant textile armor system. This type of composite armor system enables both projectile incident surface area amplification and a longer period of time to arrest the projectile. Typical materials include ceramics for a hard front face and a textile fabric system to arrest the projectile. These types of systems have mass efficiencies over four times greater than traditional steel armor systems (rolled homogeneous armor). Issues with ceramic/textile armor systems are typically related to fracture from mishandling and limited multi-hit performance. In summary approaches that can address both amplification of projectile surface area and an increase in the time duration to arrest or projectile will greatly improve the mass efficiency of the armor system.

D. DUAL-HARDNESS TITANIUM ARMOR

In 1974, Roger Perkins at Lockheed Missiles and Space Company, published an extensive report on dual-hardness titanium armor for the Army Materials and Mechanics Research Center. He found that "a dual-hardness titanium armor consisting of a Ti3Si3Fe0.5N hard-face alloy bonded to a Ti7Al2.5Mo back-face alloy provides good protection against 30-cal AP threats at low areal densities (6 to 8 lbs/ft^2)" [2]. The armor concept was shown to be more effective than homogeneous titanium alloy armor. Perkins also reported that the key factor governing the ballistic limit of dual-hardness titanium armor is surface hardness, which must exceed Rockwell C 60 before it becomes more effective than commercial steel armors.

E. TITANIUM SURFACE COATING TREATMENTS

Surface engineering techniques may be applied to titanium alloys to improve performance for various applications. To this end, methods exist in three main categories: heat treatment, coatings, and thermochemical treatment. This research makes use of a coating technique called physical vapor deposition (PVD).

PVD is a blanket term that encompasses several process (including evaporation, ion plating, and sputtering) to deposit ceramics, alloys, or metastable materials on a wide variety of substrates [3]. A relevant application is using PVD for the coating of tool material with titanium nitride in order to lengthen the lifetime of the tool through decreased wear. Usually, this is accomplished through reactive ion plating or reactive sputtering.

F. FORMING OF TITANIUM AND TITANIUM ALLOYS

This thesis examines two types of titanium in particular: Titanium Grade 2 (G2) which is over 99% pure, and titanium grade 5 (Ti6Al4V), a much harder, alpha-beta alloy. Ti6Al4V is the most widely used titanium alloy, accounting for about 60% of all titanium production [4].

In the manufacture of body armors, wearability must be considered. That is, the armor system must conform comfortably to the wearer’s natural contours and cannot be simply a flat plate. Thus, formability should be considered. Titanium and titanium alloys were considered for this application because they exhibit the unique property called superplasticity. Superplastic materials, like Ti6Al4V, can be formed to over 1000% elongation without succumbing to the harmful effects of necking or material property changes. Some of titanium’s superplastic characteristics are tabulated in Table 1.

Table 1. Superplastic characteristics of titanium alloys. Adapted from [4].

Alloy	Test Temperature		Strain rate,1/s	Strain-rate sensitivity factor, m	Elongation, %
	°C	°F			
Commercially pure titanium	850	1560	17E-4	…	115
Ti6Al4V	840-870	1545-1600	1.3E-4 to E-3	0.75	750-1170

THIS PAGE INTENTIONALLY LEFT BLANK

III. EXPERIMENTATION AND MODELING

A. EXPERIMENTAL SETUP

Ballistic tests were conducted at an NPS gun range facility setup at the Naval Surface Warfare Center in Dahlgren, Virginia. Within the facility, a Mann barrel gun system is used to launch projectiles against armor coupons at controlled positions and orientations. The incident projectile velocity is measured using four Ohler IR break screens and knowledge of both time of arrival and screen separation distances. A schematic of this configuration is shown in Figure 2.

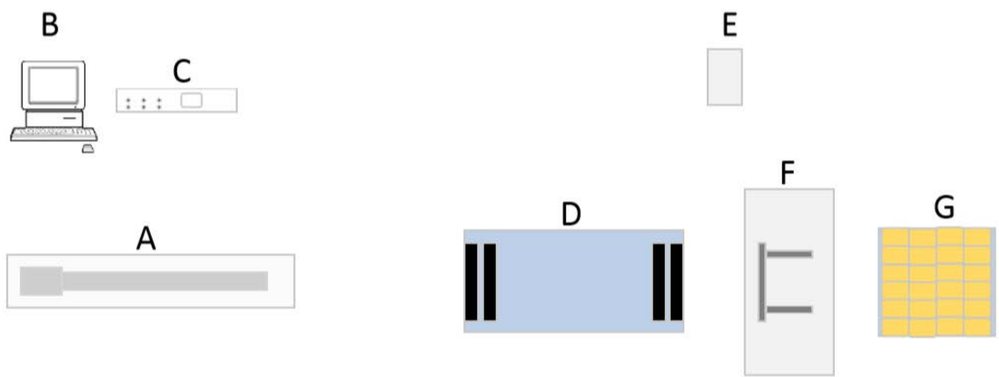

(A) Mann barrel gun system; (B) computer and data acquisition interface; (C) remote, manual trigger; (D) velocity screens; (E) high speed video camera; (F) mounting stand; (G) sand-filled box to catch projectile and spall [5].

Figure 2. Schematic of ballistic test setup. Source: [5].

The impact velocity is controlled by the amount and type of gun powder placed in each projectile casing. The powder was carefully measured and correlated to the required impact velocity (2450 feet/second). Each of the tested targets was backed by two 1-inch-thick polycarbonate blocks (areal dimensions 4" x 4"). The polycarbonate blocks served to gauge the penetration depth for the targets that failed to stop the incident bullet. A prepared target with polycarbonate backing is shown in Figure 3.

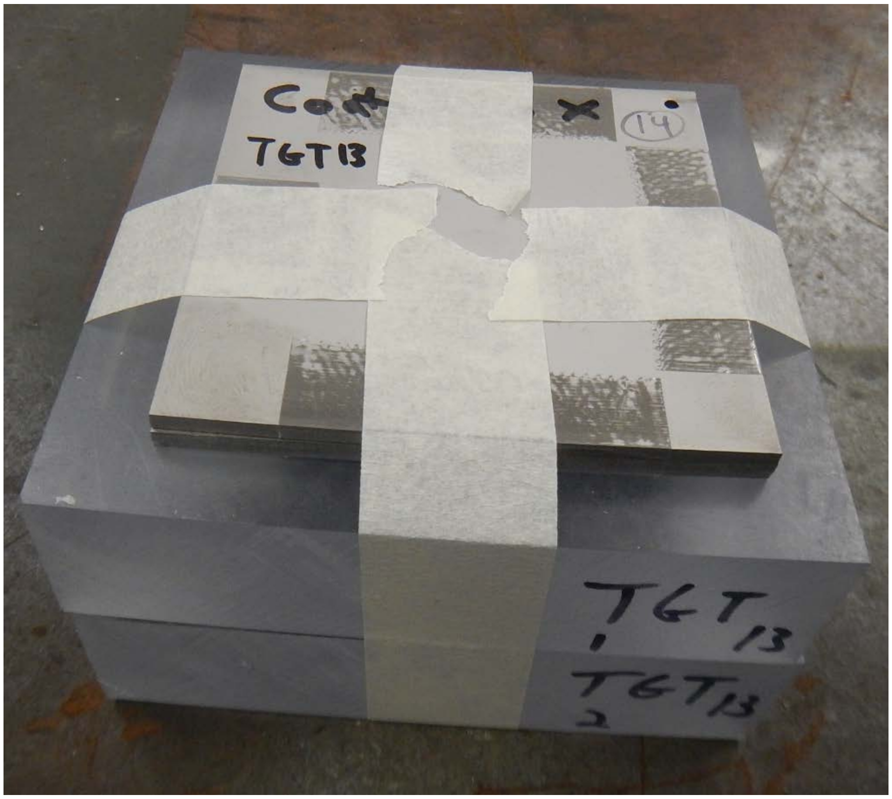

Targets were held together by common clear/masking tape, which has a negligible effect on ballistic performance. Assemblies like this one were then affixed to the mounting stand using duct tape.

Figure 3. Prepared target assembly with polycarbonate blocks

B. TARGET DESIGN AND FABRICATION

To determine the optimal design for a titanium armor system, several target configurations were prepared and tested. Each of the targets were 3-inch by 3-inch squares and had overall thicknesses equal to or less than 8 millimeters and an overall areal density under 5lbs/ft^2, as required by the design constraints (see I.B.1). The following list summarizes the approaches considered during this research.

- Monolithic plates
- Homogeneous laminate systems
- Heterogeneous laminate systems
- Hard front face systems

    - Ceramic
    - Thin coatings varied thickness
        - TiB_2
        - TiN
        - AlTiN
- Ceramic ball front face
- Fiber backing systems

Homogeneous and heterogeneous laminate systems are described together as "dual-hardness laminae."

1. Dual-Hardness Laminae

This approach comprises multiple thin layers of Ti6Al4V and titanium grade 2 (G2) arranged in various configurations, to include alternating laminae, totaling no more than 8 millimeters in thickness and an areal density not to exceed 5lbs/ft^2.

The idea being explored here is that the harder Ti6Al4V layers will blunt the projectile, providing a wider surface area of interaction between the projectile and the target, thus decreasing pressure, while the softer, purer G2 layers will absorb the impact by more readily undergoing plastic deformation and spread the force over a larger surface area [6]. Figure 4 is a diagram of this system.

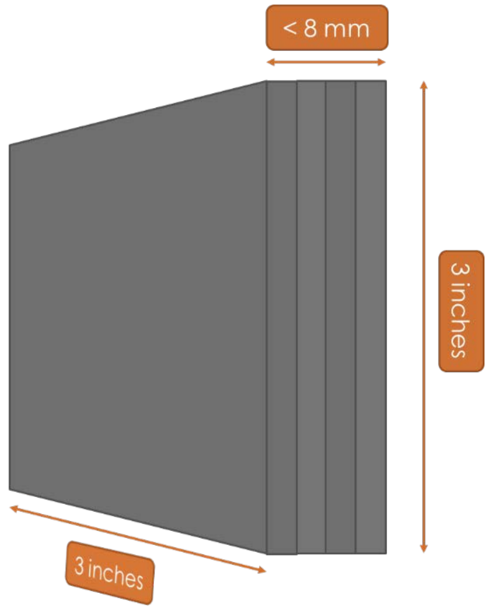

Figure 4. Dual-hardness titanium laminae

2. Ceramic and Titanium Plates

For this approach, the same concepts are employed as in the dual-hardness laminar system. The front layer is a thin ceramic plate intended to blunt the bullet's ogive while the ceramic layers behind that are expected to absorb the impact. Figure 5 is a diagram of this system. The front hard surface will enable an increased surface area on the projectile enabling the softer titanium alloy to perform more work against the incident target.

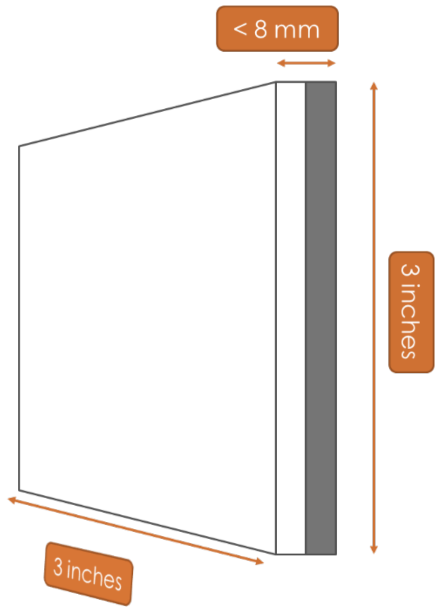

Figure 5. Ceramic and titanium plates

3. Ceramic Surface Coatings

Targets prepared for this approach are composed of Ti6Al4V that have been treated with a thin layer of a ceramic coating as opposed to entire plates. Behind the coated plate is an untreated Ti6Al4V plate. Figure 6 is a diagram of this system.

The surface coatings were applied by Kyocera Hardcoating Technologies Ltd using physical vapor deposition (PVD). Three types of ceramic were tested: titanium diboride (TiB_2), aluminum titanium nitride (AlTiN), and titanium nitride (TiN).

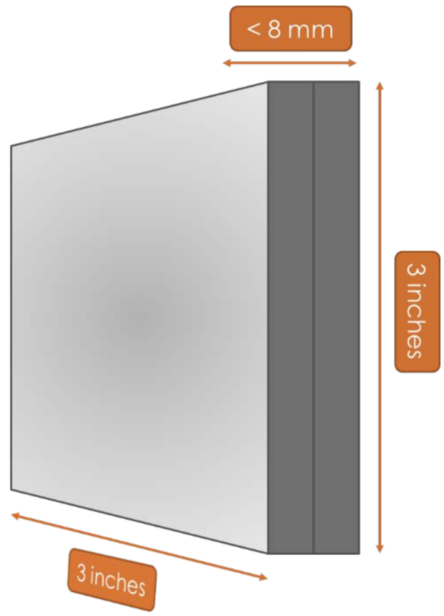

Figure 6. Ceramic surface coatings

a. Titanium Diboride (TiB_2)

Titanium diboride is an extremely hard ceramic used for various specialized applications including use in cutting tools, crucibles, and most notably, impact resistant armor. Because it does not exist in nature, TiB_2 must be synthesized. Thin films of TiB2 can be applied to substrates via PVD, chemical vapor deposition (CVD), or electroplating. For these samples, the Ti6Al4V plates were coated using PVD in up to six layers of 2 microns each. From Kyocera's website [7], some characteristics of TiB_2 coatings are tabulated in Table 2.

Table 2. Material properties of titanium diboride. Adapted from: [7].

Coating	**TiB_2**
Color	Light Gray
Structure	Graded
Microhardness	4000 HV
Density	4.52 g/cm^3

b. Titanium Nitride (TiN)

Titanium nitride is an extremely hard ceramic used for coating tools and surfaces that may otherwise experience significant wear during their lifetime. Because of its biostability, TiN is often used in medical implants and protheses. These samples were prepared with a thickness of 4 microns using PVD. Some characteristics of TiN coatings are tabulated in Table 3.

Table 3. Material properties of titanium nitride. Adapted from [7].

Coating	**TiN**
Color	Gold
Structure	Multi-layered
Microhardness	2200HV 0.05
Density	5.40 g/cm^3

c. Aluminum Titanium Nitride (AlTiN)

Aluminum titanium nitride or titanium aluminum nitride (TiAlN, for variations containing less than 50% Al) are an improved version of TiN for hardening the surface of tools. It exhibits both higher resistance to oxidation, and increased hardness compared to TiN. AlTiN coatings are almost always applied using PVD, specifically cathodic arc deposition. These samples were prepared in the standard manner with a film thickness of 4 microns. Some characteristics of AlTiN coatings are tabulated in Table 4.

Table 4. Material properties of aluminum titanium nitride. Adapted from [7].

Coating	**Aluminum Titanium Nitride**
Color	Dark Gray-Black
Structure	Graded
Microhardness	3300HV 0.05
Density	5.22 g/cm^3

4. Ceramic Balls

This approach involves the use of a Ti6Al4V plate as a substrate for a high tensile strength (7000 psi) polyurea encapsulating close-packed ceramic spheres. The spheres are made of either Alumina (Al_2O_3) or Silicon Carbide (SiC). The spheres range in diameter from 7/32" to 1/8." The objective here was to make use of a hard ceramic front face for blunting the projectile while using the Ti as a spall catcher on the back side. Figure 7 is a diagram of this system.

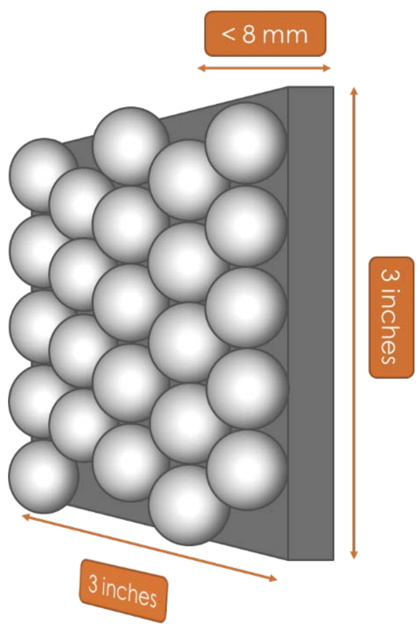

Figure 7. Ceramic balls (Polyurea not shown)

5. Fiber-Backed System

Targets prepared for this approach comprised a Ti64AlV plate backed by a multilayered fibrous composite. The composite was made of Ultrahigh Molecular Weight Polyethylene (UHMWPE) (Spectrashield 3136) sheets that were heated to 135 ℃ and pressed together at 3000 psi, making for a rigid, but comparatively lightweight (<1g/cm^3) textile layer capable of absorbing kinetic energy of a projectile. Figure 8 is a diagram of this system.

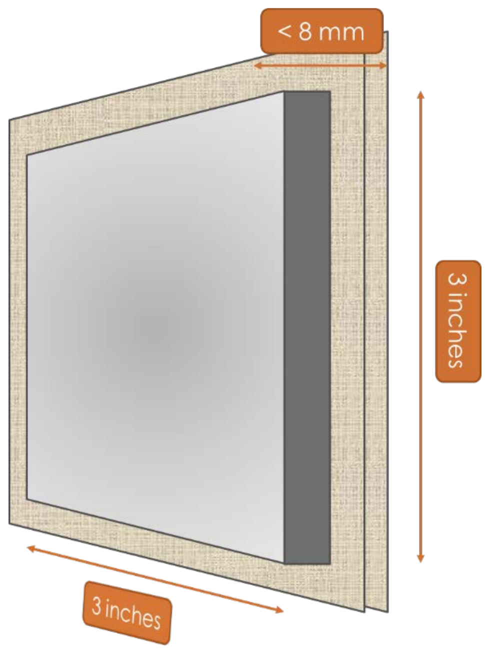

Figure 8. Fiber-backed system

C. COATING HARDNESS MEASUREMENT

Because hardness is such an important material characteristic in impact dynamics, several evaluations were made on the ceramic coated Ti6Al4V samples. The samples, coated in either TiB_2 (of 1, 2, 4, or 6 layers), TiN, or AlTiN were tested using 3 common methods: Brinell, Rockwell C, and Vickers Micro-indentation. A less common method called Nanoindentation was also used to test the surface hardness of TiB_2 (of 2 layers), TiN, and AlTiN.

1. **Brinell**

The Brinell hardness scale is one of many definitions of hardness used in material science. It makes use of a spherical tungsten indenter that is applied to a surface with a known force (shown in Figure 9). After the load is removed, the diameter of the remaining indentation (left through plastic deformation) is measured under a magnifying glass. The Brinell Hardness (HBW) is then calculated with the following equation:

$$HBW = 0.102\frac{2F}{\pi D(D - \sqrt{D^2 - d^2})}$$

where F is the applied load in Newtons, D is the diameter of the indenter, and d is the diameter of the indentation. This resulting number, which is unitless thanks to the leading coefficient, is used to describe the relative hardness of the material.

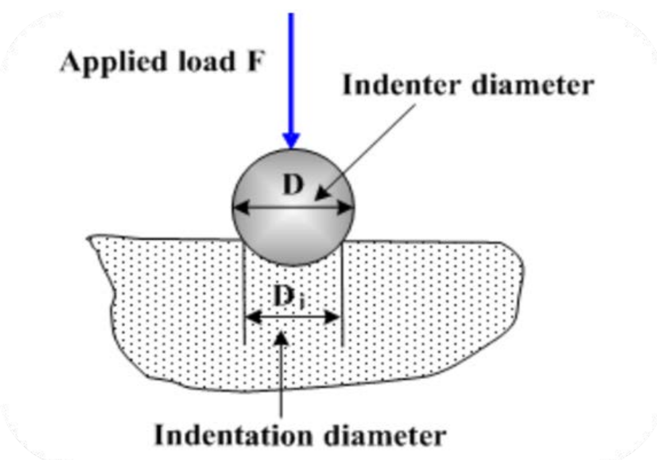

Image licensed by Creative Commons; obtained through a Microsoft Office image search, June 2018.

Figure 9. Brinell hardness test

2. Rockwell C

Unlike Brinell, the Rockwell hardness scale uses penetration depth, not indentation size, to measure surface hardness. It makes use of a spherical or conical indenter which is applied to a sample with a small "pre-load" followed by a larger load. One of several Rockwell scales, the "C" scale uses a 120° sphero-conical, hardened steel (sometimes diamond tipped) indenter and a 150 kgf load. Figure 10 is a diagram of this test.

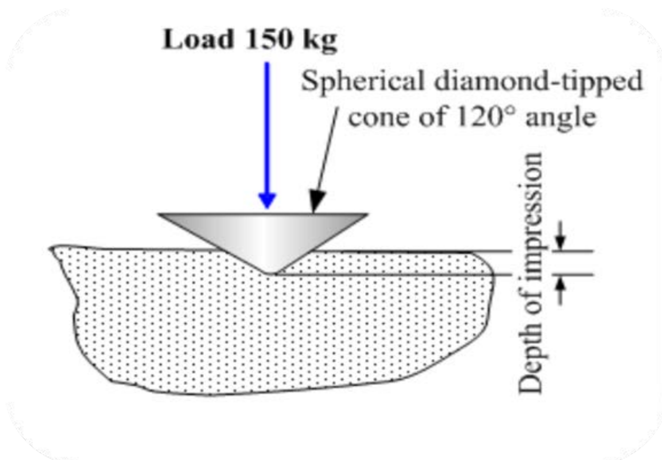

Image licensed by Creative Commons; obtained through a Microsoft Office image search, June 2018.

Figure 10. Rockwell C hardness test

3. Vickers Micro-indentation

The Vickers hardness scale is similar to Brinell in that it uses indentation size to determine surface hardness, but instead of a spherical tungsten indenter, it makes use of a diamond in the shape of a 136° square-based pyramid. The indentation is then measured across opposing corners and the following equation is used to calculate Vickers hardness (HV):

$$HV = \frac{F}{A} \approx \frac{1.8544F}{d^2}$$

where *F* is the applied load in kilograms force, and *d* is the diagonal distance between corners in millimeters. Microhardness, as measured by a Vickers micro-indenter, has much shallower penetration depths than those of the methods previously discussed, and the indention can only be viewed using a microscope. Figure 11 is a diagram of this process.

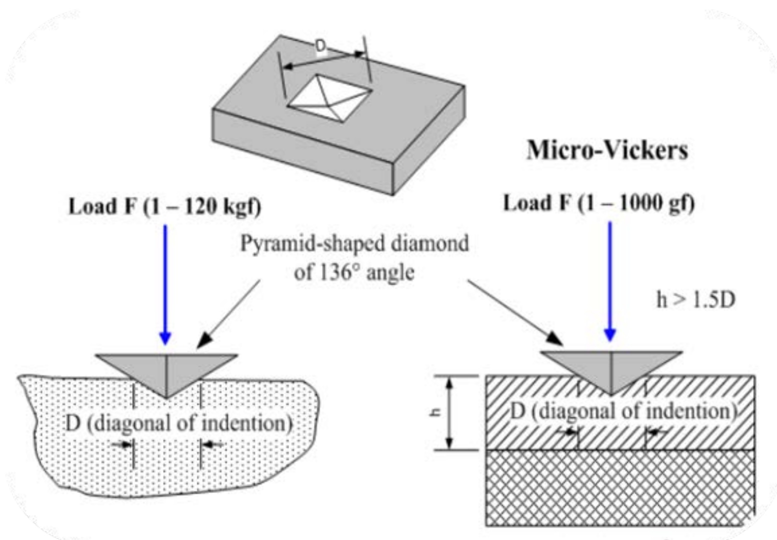

Image licensed by Creative Commons; obtained through a Microsoft Office image search, June 2018.

Figure 11. Vickers microhardness test

4. Nanoindentation

Because surface coatings can be extremely thin, a method of measuring hardness must be employed which does not penetrate past the layer. Nanoindentation is essentially an even more precise, computer-controlled version of the Vickers Microhardness testing. Measurement with a nanoindenter is highly automated and makes use of a tiny diamond tip that can be one of many various shapes. Due to the small indentation area, which can be on the order of microns or even nanometers, accurate testing requires that the surface of the sample be well polished. KLA-Tencor's Nano Indenter G200 (Figure 12) was used for this particular experiment.

Figure 12. Nano Indenter G200. Source: [8].

D. COMPUTATIONAL MODELS

As with most research, coupling of both experimental and theoretical studies can enable a better understanding of an event. Within this study, initial ballistic impacts of the titanium laminate systems were used to anchor hydrocode modeling.

Computer simulations can be an informative tool in penetration studies because they can provide highly detailed material stress information. Through parallel efforts with experimentation, a grounding of experimental results to modeling parameters can be performed. More important predictive capabilities anchored on experimental comparisons can occur. During this research, a simulation code known as CTH was employed to investigate specific phenomena and make predictions about ballistic performance of various armor systems.

1. CTH

Developed by Sandia National Laboratory, CTH is a “multi-material, Eulerian, large deformation, strong shock wave, solid mechanics code” [9]. It is capable of producing time-variable two and three-dimensional models of visco-plastic, multiphase, elastic, porous and explosive materials. CTH comes with hundreds of built in material definitions and includes equation of state models.

As a government owned export controlled software, distribution is limited to U.S. citizens and requires licensure from Sandia National Laboratory.

The code, built in both FORTRAN and C, is designed to run on most mainstream operating systems. For this research, text format input files were written and run using a desktop workstation with Windows 7. Due to the sheer number of advanced calculations that CTH makes during simulation, work must be limited in detail so as to avoid overburdening the machine. Thus, models were limited to two dimensions for these studies.

It should be noted that by default, CTH uses a centimeter-gram-second (cgs) system of units and all descriptions of the simulation created therein will follow accordingly.

2. Projectile Modeling

In order to achieve realistic simulations, an accurate model of the penetrator had to be developed. The 7.62x39mm ball round (discussed in section I.B.2) was first recreated in SolidWorks with accurate material definitions so that the built in mass analysis functionality could be leveraged, and thus dimensional accuracy could be verified. This model, shown in Figure 13, was initially created with the intention of be uploaded to CTH (through a proprietary software known as Cubit) and simulated in three dimensions. Unfortunately, as previously mentioned, the workstation was unable to handle the calculations.

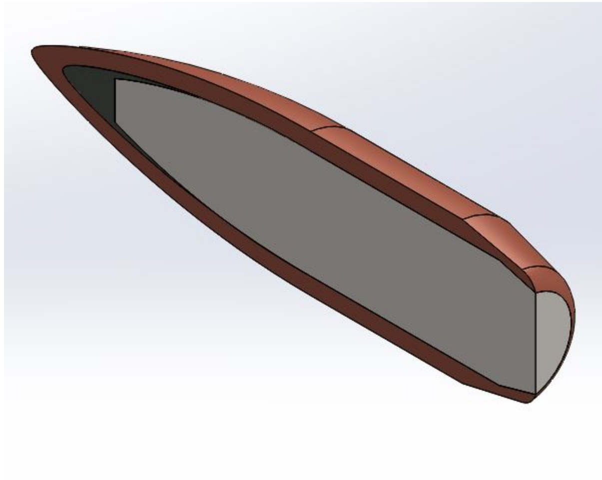

Figure 13. Cutaway of SolidWorks model

Consequently, work began on creating a two-dimensional model using CTH's built-in geometry functions (Figure 14). As the model was iteratively refined to accurately reflect the dimensions of the bullet, a note-worthy trend was observed through interim penetration simulations. A bullet of appropriate dimensions made entirely of steel was a less effective penetrator for titanium targets than a bullet with a more realistic anatomy (steel core, lead filler, and copper casing). Presumably this is due to the "lubricating" effect that the softer outer materials have between the steel core and the titanium target during hydrodynamic flow (see section II.A.). Alternatively, this could be a product of an increased core cross-section and thus a larger impact area (see II.C.).

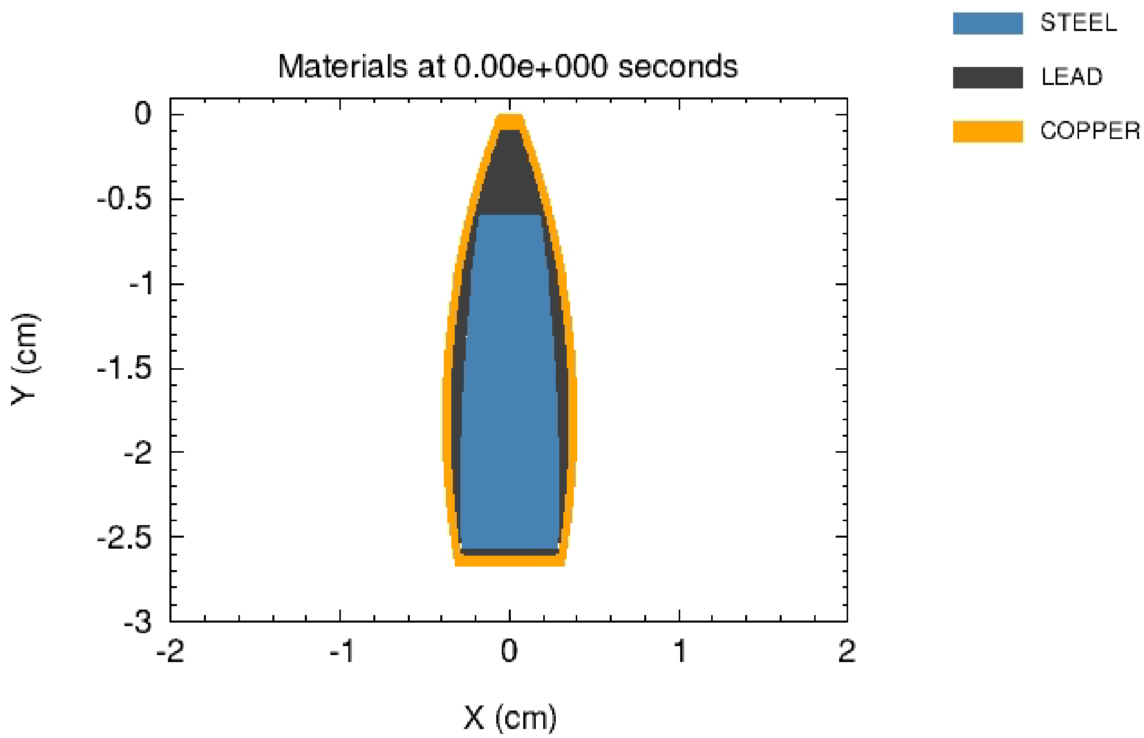

Figure 14. CTH-generated bullet model

The simulated bullet is composed of three parts: steel core, lead filler, and a copper jacket. The steel core is a near-cylindrical, blunted ogive of length 1.99 cm and radius 0.29 cm. Its material equation of state (EOS) is defined by 100STEEL_TEP of the Mie-Gruneisen (MGR) model and its strength is defined by STEEL of the Johnson-Cook Strength (JO) model. The lead filler is a hollow ogive shape with an outer radius of 0.35 cm and a length appropriate to fill the gap between the core and the jacket. Its material EOS is defined by LEAD of the MGR model and its strength is defined by LEAD of the Steinberg-Guinan-Lund (ST) model. Finally, the copper jacket is a hollow ogive shape (curvature radius 5 cm) with a length of 2.67 cm and an outer radius of 0.4 cm. These dimensions agree with those of an actual 7.62x39mm bullet to within a hundredth of a centimeter. The material EOS is defined by Ti6AL4V of the MGR model and its strength side fined by COPPER of the JO model. Descriptions of these material models can be found in the CTH user manual, distributed by Sandia National Laboratory [10].

3. Laminate Studies

A series of simulations were conducted to determine if CTH could realistically model the ballistic behavior of laminar armor systems. Three input files were created that closely resembled experimental conditions so that the results could be compared to those of the ballistics tests. Each scenario involved a 7.62x39mm ball round impacting a 0.25" (0.635 cm) thick Ti6Al4V target at 750 m/s (approximately muzzle velocity). The targets were each backed with a 1" polycarbonate (LEXAN) block and a large steel backboard and are described as follows:

- 1 Ti6Al4V plate of thickness 0.25" (0.635 cm)
- 2 Ti6Al4V plates of thickness 0.125" (0.3175 cm) each
- 8 Ti6Al4V plates of thickness 0.03125" (0.079375 cm) each

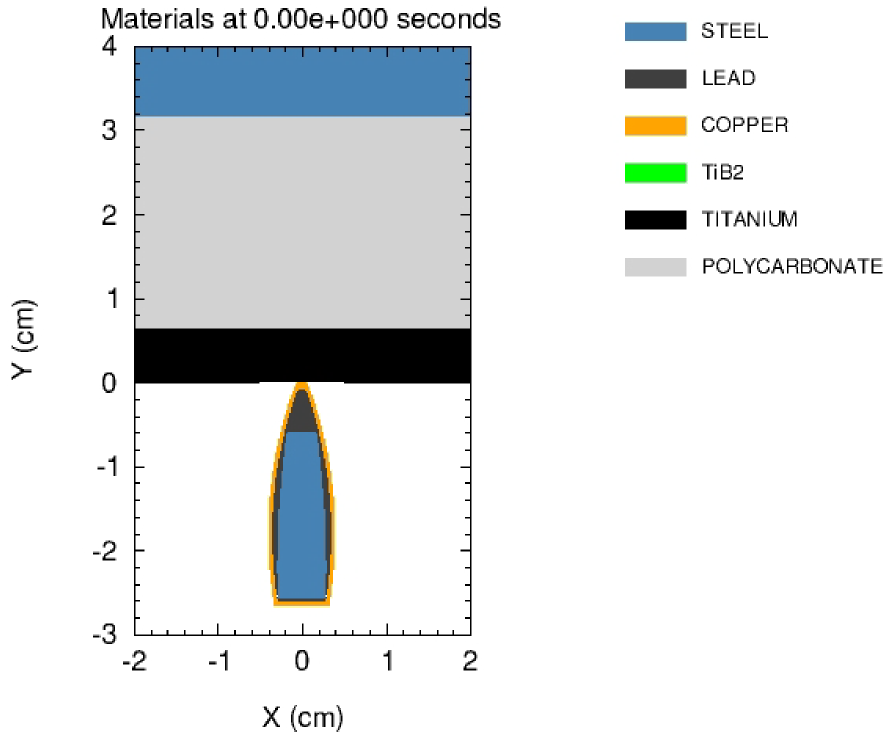

Figure 15. Starting position of materials in CTH simulation for laminate studies

4. Coating Studies

A series of simulations were conducted to determine what effect, if any, a film of ceramic would have on the stopping power of a Ti6Al4V target and at approximately what thickness would it be useful. In particular, this study examines the relationship between ceramic coating thickness and dilation of the steel core's front face (see II.C). TiB_2 was used for this study because its material properties were already well defined in CTH.

Each scenario involved a 7.62x39mm ball round impacting the target at 750 m/s (~ muzzle velocity AK-47). The targets were comprised of two Ti6Al4V plates and a layer of TiB_2 on the front face. Holding the total target thickness constant at 0.55232 cm in total thickness (5 lb/ft^2 areal density), the thickness of the ceramic front face was increased (and the thickness of the Ti6Al4V plate was decreased) by 0.01 cm for run and data was recorded respectively.

No PC backing was used for this simulation so that final projectile velocity could be examined. Instead, the target width was extended to 2000 cm (effectively infinite) to render it stationary.

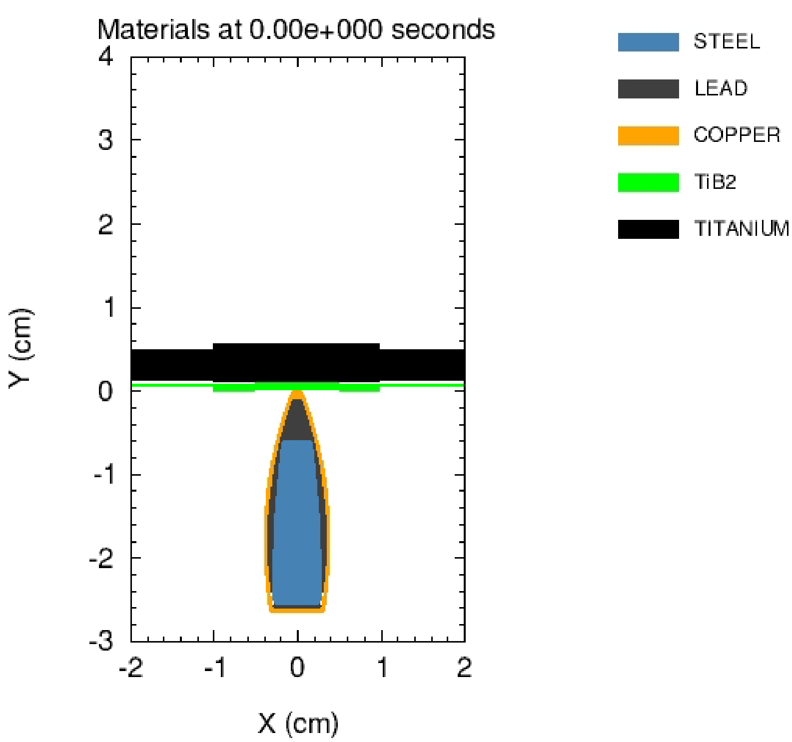

Figure 16. Starting position of materials in CTH simulation for coating studies

IV. EXPERIMENTAL DATA

As outlined in the previous chapter, experiments were conducted in a consistent manner. Targets representing variations of each of the five design approaches were prepared and shot. The four test series are numbered in chronological order, the first of which represents a wide variety of target configurations and variables (Figure 17). Each successive test series represents a narrower focus on iterations of the higher-performing configurations along with yet untested design approaches. Within this chapter, brief descriptions of the objectives, and tables of performance data are provided for each test series.

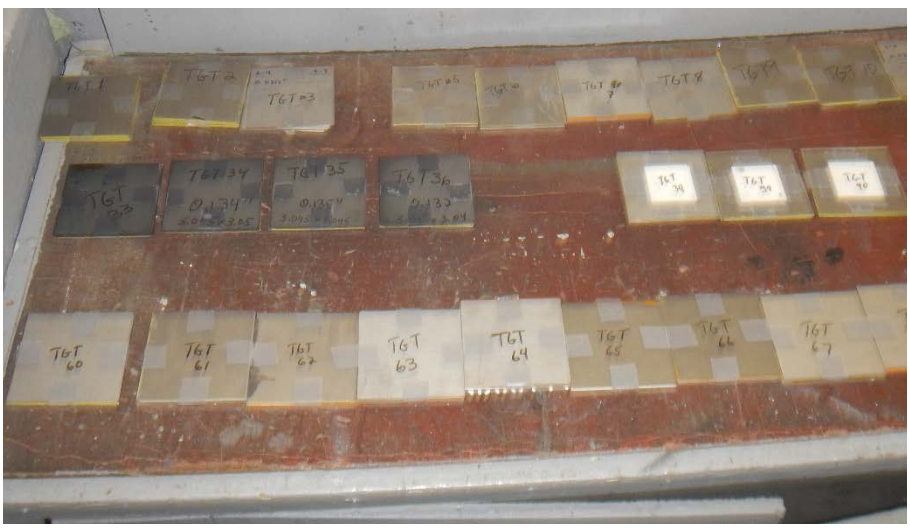

Figure 17. Prepared targets

Also detailed in this chapter are results of surface material evaluations for the ceramic-coated targets and data obtained from CTH simulations.

A. TEST SERIES 1

This test series was the largest and widest ranging of the four. The objective was to examine the effects, if any, of changes in target material, laminae thickness, and laminae order with the purpose of directing subsequent research toward promising solutions. As shown if Figure 17, Nearly 130 targets were prepared for this set with a focus on dual-hardness laminae (see III.B.1) and ceramic/titanium plate (see III.B.2) systems.

The data table was split into sections (Tables 5–10) specific to the target configuration being studied. Figures in the "Penetration Depth" column denote depth of penetration into the polycarbonate blocks (described in III.A). Note that the polycarbonate blocks represent a measure of the residual energy of the target system when complete penetration of the titanium target occurs to enable a relative comparison of the penetration resistance performance. The term homogeneous is used to describe targets with laminae that are adjacent to laminae of the same material, whereas heterogeneous describes dual-hardness targets with alternating (Ti6Al4V and G2) laminae.

Table 5. Test series 1: Titanium grade 2 monolithic

Target #	Target Description	Areal density (lb/ft2)	Thickness (in)	Velocity (ft/s)	Penetration Depth
96.	1 x 0.125" G2	2.86848	0.1245	2443	> 2"
97.	1 x 0.15" G2	3.744	0.1625	2412	> 2"
98.	1 x 0.15" G2	3.744	0.1625	2422	> 2"
101.	1 x 0.25" G2	5.8176	0.2525	2420	1.95"
102.	1 x 0.25" G2	5.95584	0.2585	2333	> 2"
105.	1 x 0.313" G2	7.68384	0.3335	2361	1.194
106.	1 x 0.313" G2	7.56864	0.3285	2510	1.357

Table 6. Test series 1: Titanium grade 2 laminar homogeneous

Target #	Target Description	Areal density (lb/ft2)	Thickness (in)	Velocity (ft/s)	Penetration Depth
1.	7 x 0.032" G2	5.2812	0.225	2489	2"
2.	7 x 0.032" G2	5.433768	0.2315	2479	> 2"
5.	1 x 0.09" G2 1 x 0.032" G2 1 x 0.09" G2	5.140368	0.219	2402	> 2"
6.	1 x 0.09" G2 1 x 0.032" G2 1 x 0.09" G2	5.199048	0.2215	2472	> 2"
77.	8 x 0.032" G2	5.762376	0.2455	2435	> 2"
78.	8 x 0.032" G2	5.891472	0.251	2438	> 2"
81.	9 x 0.032" G2	6.583896	0.2805	2423	> 2"
82.	9 x 0.032" G2	6.583896	0.2805	2426	> 2"
85.	10 x 0.032" G2	7.323264	0.312	2437	> 2"
86.	10 x 0.032" G2	7.499304	0.3195	2446	> 2"
119.	2 x 0.125" G2	5.856264	0.2495	2300	> 2"
120.	2 x 0.125" G2	5.832792	0.2485	2511	> 2"
121.	2 x 0.15" G2	7.675344	0.327	2272	1.609"
122.	2 x 0.15" G2	7.616664	0.3245	2371	> 2"
125.	2 x 0.25" G2	11.97072	0.51	2389	0
126.	2 x 0.25" G2	11.653848	0.4965	2415	0

Table 7. Test series 1: Titanium grade 5 (Ti6AlV) monolithic

Target #	Target Description	Areal density (lb/ft2)	Thickness (in)	Velocity (ft/s)	Penetration Depth
109.	1 x 0.15" G5	3.708576	0.158	2489	> 2"
110.	1 x 0.15" G5	3.661632	0.156	2327	> 2"
111.	1 x 0.16" G5	4.51836	0.1925	2535	> 2"
112.	1 x 0.16" G5	4.483152	0.191	2570	0.55"
113.	1 x 0.25" G5	5.938416	0.253	2533	> 2"
114.	1 x 0.25" G5	6.008832	0.256	2521	> 2"
115.	1 x 0.28" G5	6.771672	0.2885	2402	0"
116.	1 x 0.28" G5	6.818616	0.2905	2524	0.33
117.	1 x 0.313" G5	7.604928	0.324	2489	1"
118.	1 x 0.313" G5	7.546248	0.3215	2503	1"

Table 8. Test series 1: Titanium grade 5 (Ti6Al4V) laminar homogeneous

Target #	Target Description	Areal density (lb/ft2)	Thickness (in)	Velocity (ft/s)	Penetration Depth
3.	7 x 0.032” G5	5.39136	0.234	2399	1”
4.	7 x 0.032” G5	5.3568	0.2325	2475	1.449”
7.	1 x 0.09” G5 1 x 0.032” G5 1 x 0.09” G5	5.05728	0.2195	2361	1.196”
8.	1 x 0.09” G5 1 x 0.032” G5 1 x 0.09” G5	5.08032	0.2205	2438	> 2”
79.	8 x 0.032” G5	5.94432	0.258	2458	0.756”
80.	8 x 0.032” G5	6.03648	0.262	2455	0.684”
83.	9 x 0.032” G5	6.77376	0.294	2465	0.125”
84.	9 x 0.032” G5	6.63552	0.288	2435	0.125”
87.	10 x 0.032” G5	7.47648	0.3245	2441	0.0”
88.	10 x 0.032” G5	7.58016	0.329	2446	0.0”
127.	2 x 0.125” G5	5.78304	0.251	2448	0.0”
128.	2 x 0.125” G5	5.79456	0.2515	2428	0.0”
129.	2 x 0.15” G5	7.24608	0.3145	2425	0.0”
130.	2 x 0.15” G5	7.2576	0.315	2431	0.0”
131.	2 x 0.16” G5	8.88192	0.3855	2412	0.0”
132.	2 x 0.16” G5	8.85312	0.38425	2415	0.0”
133.	2 x 0.25” G5	11.7504	0.51	2428	0.0”
134.	2 x 0.25” G5	11.68128	0.507	2422	0.0”

Table 9. Test series 1: Titanium grade 5 (Ti6Al4V) and titanium grade 2 laminar heterogeneous

Target #	Target Description	Areal density (lb/ft2)	Thickness (in)	Velocity (ft/s)	Penetration Depth
9.	3 x 0.032” G2 4 x 0.032” G5	5.393808	0.23225	2472	> 2”
10.	3 x 0.032” G2 4 x 0.032” G5	5.307408	0.2285	2448	> 2”
11.	3 x 0.032” G5 4 x 0.032” G2	5.391432	0.2315	2431	> 2”
12.	3 x 0.032” G5 4 x 0.032” G2	5.379696	0.231	2426	> 2”
13.	4 x 0.032” G5 3 x 0.032” G2	5.353056	0.2305	2380	> 2”
14.	4 x 0.032” G5 3 x 0.032” G2	5.458032	0.235	2345	1.386”

Target #	Target Description	Areal density (lb/ft2)	Thickness (in)	Velocity (ft/s)	Penetration Depth
15.	4 x 0.032” G2 3 x 0.032” G5	5.354712	0.23	2396	> 2”
16.	4 x 0.032” G2 3 x 0.032” G5	5.3658	0.2305	2475	> 2”
17.	1 x 0.032” G5 1 x 0.09” G2 1 x 0.09” G5	5.20452	0.2235	2383	> 2”
18.	1 x 0.032” G5 1 x 0.09” G2 1 x 0.09” G5	5.135616	0.2205	2486	> 2”
19.	1 x 0.032” G2 1 x 0.09” G5 1 x 0.09” G2	5.12136	0.2205	2493	> 2”
20.	1 x 0.032” G2 1 x 0.09” G5 1 x 0.09” G2	5.132016	0.221	2458	> 2”
45.	1 x 0.032” G5 1 x 0.032” G2 1 x 0.032” G5 1 x 0.032” G2 1 x 0.032” G5 1 x 0.032” G2 1 x 0.032” G5	5.35392	0.2305	2490	> 2”
46.	1 x 0.032” G5 1 x 0.032” G2 1 x 0.032” G5 1 x 0.032” G2 1 x 0.032” G5 1 x 0.032” G2 1 x 0.032” G5	5.306328	0.2285	2554	> 2”
47.	1 x 0.032” G2 1 x 0.032” G5 1 x 0.032” G2 1 x 0.032” G5 1 x 0.032” G2 1 x 0.032” G5 1 x 0.032” G2	5.38992	0.2315	2465	> 2”
48.	1 x 0.032” G2 1 x 0.032” G5 1 x 0.032” G2 1 x 0.032” G5 1 x 0.032” G2 1 x 0.032” G5 1 x 0.032” G2	5.413824	0.2325	2503	> 2”
49.	1 x 0.032” G2 2 x 0.09” G5	5.060448	0.219	2484	1.9”
50.	1 x 0.032” G2 2 x 0.09” G5	4.967424	0.215	2473	> 2”

Target #	Target Description	Areal density (lb/ft2)	Thickness (in)	Velocity (ft/s)	Penetration Depth
51.	1 x 0.032" G5 2 x 0.09" G2	5.208048	0.2225	2465	> 2"
52.	1 x 0.032" G5 2 x 0.09" G2	5.23152	0.2235	2503	> 2"
53.	1 x 0.032" G2 6 x 0.032" G5	5.301936	0.2295	2479	1.50"
54.	1 x 0.032" G2 6 x 0.032" G5	5.313672	0.23	2506	1.875"
55.	2 x 0.032" G2 5 x 0.032" G5	5.316192	0.2295	2490	> 2"
56.	2 x 0.032" G2 5 x 0.032" G5	5.223384	0.2255	2446	> 2"
57.	1 x 0.032" G5 6 x 0.032" G2	5.303232	0.2265	2508	2"
58.	1 x 0.032" G5 6 x 0.032" G2	5.348664	0.2285	2505	> 2"
59.	2 x 0.032" G5 5 x 0.032" G2	5.322672	0.228	2367	> 2"
60.	2 x 0.032" G5 5 x 0.032" G2	5.205528	0.223	2486	> 2"
61.	1 x 0.032" G2 1 x 0.09" G2 1 x 0.09" G5	5.100408	0.219	2466	> 2"
62.	1 x 0.032" G2 1 x 0.09" G2 1 x 0.09" G5	5.076936	0.218	2389	> 2"
63.	1 x 0.032" G5 1 x 0.09" G5 1 x 0.09" G2	5.109624	0.22	2308	1.27"
64.	1 x 0.032" G2 1 x 0.09" G2 1 x 0.09" G5	5.086368	0.219	2327	1.285"
65.	1 x 0.09" G5 1 x 0.09" G2 1 x 0.032" G2	5.076936	0.218	2520	> 2"
66.	1 x 0.09" G5 1 x 0.09" G2 1 x 0.032" G2	5.155488	0.222	2482	> 2"
67.	1 x 0.09" G2 1 x 0.09" G5 1 x 0.032" G5	5.04108	0.2165	2360	> 2"
68.	1 x 0.09" G2 1 x 0.09" G5 1 x 0.032" G5	5.110848	0.2195	2455	> 2"

Target #	Target Description	Areal density (lb/ft2)	Thickness (in)	Velocity (ft/s)	Penetration Depth
89.	1 x 0.032” G5 1 x 0.032” G2 1 x 0.032” G5 1 x 0.032” G2 1 x 0.032” G5 1 x 0.032” G2 1 x 0.032” G5 1 x 0.032” G2	5.986584	0.2575	2465	> 2”
90.	1 x 0.032” G5 1 x 0.032” G2 1 x 0.032” G5 1 x 0.032” G2 1 x 0.032” G5 1 x 0.032” G2 1 x 0.032” G5 1 x 0.032” G2	5.943096	0.2555	2458	> 2”
91.	1 x 0.032” G5 1 x 0.032” G2 1 x 0.032” G5 1 x 0.032” G2 1 x 0.032” G5 1 x 0.032” G2 1 x 0.032” G5 1 x 0.032” G2 1 x 0.032” G5	6.633	0.2855	2438	> 2”
92.	1 x 0.032” G5 1 x 0.032” G2 1 x 0.032” G5 1 x 0.032” G2 1 x 0.032” G5 1 x 0.032” G2 1 x 0.032” G5 1 x 0.032” G2 1 x 0.032” G5	6.74712	0.2905	2455	> 2”
93.	1 x 0.032” G5 1 x 0.032” G2 1 x 0.032” G5 1 x 0.032” G2 1 x 0.032” G5 1 x 0.032” G2 1 x 0.032” G5 1 x 0.032” G2 1 x 0.032” G5 1 x 0.032” G2	7.245432	0.3115	2425	1.97”

Target #	Target Description	Areal density (lb/ft2)	Thickness (in)	Velocity (ft/s)	Penetration Depth
94.	1 x 0.032” G5 1 x 0.032” G2 1 x 0.032” G5 1 x 0.032” G2 1 x 0.032” G5 1 x 0.032” G2 1 x 0.032” G5 1 x 0.032” G2 1 x 0.032” G5 1 x 0.032” G2	7.404984	0.3185	2443	1.455”

Table 10. Test series 1: Ceramic front plate

Target #	Target Description	Areal density (lb/ft2)	Thickness (in)	Velocity (ft/s)	Penetration Depth
21.	1 x 0.065” BN 5 x 0.032” G2	4.545936	0.2255	2478	> 2”
22.	1 x 0.065” BN 5 x 0.032” G2	4.47552	0.2225	2472	> 2”
23.	1 x 0.065” BN 5 x 0.032” G5	4.581504	0.2301	2441	> 2”
24.	1 x 0.065” BN 5 x 0.032” G5	4.53312	0.228	2409	> 2”
25.	1 x 0.125” SiC 3 x 0.032” G2	4.359456	0.228	2371	1.25”
26.	1 x 0.125” SiC 3 x 0.032” G2	4.34772	0.2275	2468	1.489”
27.	1 x 0.125” SiC 3 x 0.032” G5	4.37472	0.2305	2380	0.69”
28.	1 x 0.125” SiC 3 x 0.032” G5	4.4064	0.2325	2409	0.789”
29.	1 x 0.065” BN 1 x 0.032” G5 1 x 0.032” G2 1 x 0.032” G5 1 x 0.032” G2 1 x 0.032” G5	4.573368	0.2285	2479	> 2”
30.	1 x 0.065” BN 1 x 0.032” G5 1 x 0.032” G2 1 x 0.032” G5 1 x 0.032” G2 1 x 0.032” G5	4.515336	0.226	2383	> 2”

Target #	Target Description	Areal density (lb/ft2)	Thickness (in)	Velocity (ft/s)	Penetration Depth
31.	1 x 0.065" BN 1 x 0.032" G2 1 x 0.032" G5 1 x 0.032" G2 1 x 0.032" G5 1 x 0.032" G2	4.622616	0.23	2462	> 2"
32.	1 x 0.065" BN 1 x 0.032" G2 1 x 0.032" G5 1 x 0.032" G2 1 x 0.032" G5 1 x 0.032" G2	4.52916	0.226	2462	> 2"
33.	1 x 0.125" BN 1 x 0.032" G5 1 x 0.032" G2 1 x 0.032" G5	3.769776	0.227	2468	1.285"
34.	1 x 0.125" BN 1 x 0.032" G5 1 x 0.032" G2 1 x 0.032" G5	3.781296	0.2305	2499	0.344"
35.	1 x 0.125" SiC 1 x 0.032" G2 1 x 0.032" G5 1 x 0.032" G2	4.424184	0.233	2405	0.898"
36.	1 x 0.125" SiC 1 x 0.032" G2 1 x 0.032" G5 1 x 0.032" G2	4.388616	0.2305	2321	0.946"
37.	1 x 0.05" BN 3 x 0.032" G5 2 x 0.032" G2	4.370472	0.2135	2491	2"
38.	1 x 0.05" BN 3 x 0.032" G5 2 x 0.032" G2	4.341672	0.2125	2492	> 2"
39.	1 x 0.05" BN 3 x 0.032" G2 2 x 0.032" G5	4.39776	0.214	2545	> 2"
40.	1 x 0.05" BN 3 x 0.032" G2 2 x 0.032" G5	4.498416	0.2186	2396	> 2"
41.	1 x 0.125" SiC 2 x 0.032" G5 1 x 0.032" G2	4.350888	0.2295	2365	1.223
43.	1 x 0.125" SiC 1 x 0.032" G5 2 x 0.032" G2	4.243176	0.222	2399	0.67"
69.	1 x 0.125" BN 1 x 0.09" G2	3.6950112	0.2226	2496	0.786"

Target #	Target Description	Areal density (lb/ft2)	Thickness (in)	Velocity (ft/s)	Penetration Depth
70.	1 x 0.190” SiC 1 x 0.09” G2	5.20776	0.283	2358	0.0”
71.	1 x 0.125” BN 1 x 0.09” G5	3.66336	0.2245	2478	> 2”
72.	1 x 0.190” SiC 1 x 0.09” G5	5.15232	0.283	2510	0.0”
73.	1 x 0.05” Al2O3 1 x 0.09” G2 2 x 0.032” G2	4.716576	0.208	2461	1.75”
74.	1 x 0.05” Al2O3 1 x 0.09” G2 2 x 0.032” G2	4.716576	0.208	2399	> 2”
75.	1 x 0.05” Al2O3 1 x 0.09” G5 2 x 0.032” G5	4.658688	0.20845	2481	0.771”
76.	1 x 0.05” Al2O3 1 x 0.09” G5 2 x 0.032” G5	4.60224	0.206	2425	0.574”

B. TEST SERIES 2

The objective of the second test series was to test the performance of targets with ceramic surface coatings, shown in Table 11. Targets are described by their coating chemistry (TiB_2, or AlTiN) followed by “SC” for single-coat and “DC” for double-coat. A single coating is approximately 4 microns thick, while a double coating is approximately 8 microns thick.

Additionally, a further examination of the laminar Ti6Al4V homogeneous configuration was conducted. Four uncoated targets were prepared to test if adding a foam (Polytetrafluoroethylene) gap between the Ti6Al4V plates had any effect on performance of binary targets (Table 12). Twenty-seven targets were shot in total. For these targets only one 1-inch polycarbonate block was used.

Table 11. Test series 2: Ceramic coatings

Target #	Target Description	Areal Density (lb/ft2)	Thickness (in)	Velocity (ft/s)	Penetration Depth (in)
1.	0.093” G5 TiB2 SC 0.125” G5	5.02272	0.218	2506	1”
2.	0.093” G5 TiB2 SC 0.125” G5	5.02272	0.218	2458	1”
3.	0.093” G5 TiB2 SC 0.125” G5	5.02272	0.218	2465	1”
4.	0.093” G5 AlTiN SC 0.125” G5	5.02272	0.218	2475	1”
5.	0.093” G5 AlTiN SC 0.125” G5	5.02272	0.218	2435	1”
6.	0.093” G5 AlTiN SC 0.125” G5	5.02272	0.218	2505	1”
7.	0.093” G5 TiB2 DC 0.125” G5	5.02272	0.218	2445	0.5”
8.	0.093” G5 TiB2 DC 0.125” G5	5.02272	0.218	2468	1”
9.	0.093” G5 TiB2 DC 0.125” G5	5.02272	0.218	2448	0.98”
10.	0.093” G5 AlTiN DC 0.125” G5	5.02272	0.218	2441	0.5”
11.	0.093” G5 AlTiN DC 0.125” G5	5.02272	0.218	2438	1”
12.	0.093” G5 AlTiN DC 0.125” G5	5.02272	0.218	2472	1”
13.	0.093” G5 TiB2 SC 0.033 G5 0.093” G5 TiB2 SC	5.04576	0.219	2448	1”
14.	0.093” G5 TiB2 SC 0.033 G5 0.093” G5 TiB2 SC	5.04576	0.219	2445	1”

Target #	Target Description	Areal Density (lb/ft2)	Thickness (in)	Velocity (ft/s)	Penetration Depth (in)
15.	0.093” G5 TiB2 DC 0.033 G5 0.093” G5 TiB2 DC	5.04576	0.219	2451	1”
16.	0.093” G5 TiB2 DC 0.033 G5 0.093” G5 TiB2 DC	5.04576	0.219	2462	1”
17.	0.093” G5 AlTiN SC 0.033 G5 0.093” G5 AlTiN SC	5.04576	0.219	2468	1”
18.	0.093” G5 AlTiN SC 0.033 G5 0.093” G5 AlTiN SC	5.04576	0.219	2458	1”
19.	0.093” G5 AlTiN DC 0.033 G5 0.093” G5 AlTiN DC	5.04576	0.219	2428	1”

Table 12. Test series 2: Titanium grade 5 (Ti6Al4V) laminar homogeneous

Target #	Target Description	Areal Density (lb/ft2)	Thickness (in)	Velocity (ft/s)	Penetration Depth (in)
21.	0.093” G5 0.125” G5	5.02272	0.218	2451	1”
22.	0.093” G5 0.125” G5	5.02272	0.218	2455	0.5”
23.	0.093” G5 0.02 PTFE 0.125” G5	5.25162	0.238	2438	1”
24.	0.093” G5 0.02 PTFE 0.125” G5	5.25162	0.238	2423	1”
25.	0.093” G5 0.094” PTFE 0.125” G5	6.09855	0.312	2431	1”
26.	0.093” G5 0.094 PTFE 0.125” G5	6.09855	0.312	2445	1”

Target #	Target Description	Areal Density (lb/ft2)	Thickness (in)	Velocity (ft/s)	Penetration Depth (in)
27.	0.777 G5 x 3	5.370624	0.2331	2465	0.9”
28.	0.777 G5 x 3	5.370624	0.2331	2449	0.9”

C. TEST SERIES 3

The third test series was an extension of the second test series. Within this test series two key studies were performed: verification of the 0.125” G5 bilayer performance and thicker coating studies. The first effort studied the performance of the 0.125” G5 bilayer performance as a function of the quantity of 1” polycarbonate backing plates. Several identical binary Ti6Al4V targets were shot, three with single 1” thickness polycarbonate blocks and three with two 1” polycarbonate blocks, shown in Table 13.

Ceramic coatings were again examined, but this time TiN and thicker TiB_2 coatings were tested. Targets coated with TiB_2 are described as either “4 coat” (16 microns thick) or “6 coat” (24 microns thick). Targets coated with TiN were all single-coat. Table 14 tabulates the results.

Table 13. Test series 3: Binary titanium grade 5 (Ti6Al4V) with varying polycarbonate thickness

Target #	Target Description	Areal Density (lb/ft2)	Thickness (in)	Velocity (ft/s)	Penetration Depth (in)
1.	2 x 0.125 G5 2” PC	5.76	0.25	2425	0.0”
2.	2 x 0.125” G5 2” PC	5.76	0.25	2455	0.0”
3.	2 x 0.125” G5 2” PC	5.76	0.25	2466	0.0”
4.	2 x 0.125” G5 1” PC	5.76	0.25	2437	0.0”
5.	2 x 0.125” G5 1” PC	5.76	0.25	2458	0.0”
6.	2 x 0.125” G5 1” PC	5.76	0.25	2451	0.0”

Table 14. Test series 3: Ceramic coatings

Target #	Target Description	Areal Density (lb/ft2)	Thickness (in)	Velocity (ft/s)	Penetration Depth (in)
7.	1 x 0.93” G5 TiN 1 x 0.125” G5	5.02272	0.218	2482	> 2”
8.	1 x 0.93” G5 TiN 1 x 0.125” G5	5.02272	0.218	2462	> 2”
9.	1 x 0.93” G5 TiN 1 x 0.125” G5 1	5.02272	0.218	2469	> 2”
10.	1 x 0.93” G5 TiB2 4 coat 1 x 0.125” G5	5.02272	0.218	2438	1”
11.	1 x 0.93” G5 TiB2 4 coat 1 x 0.125” G5	5.02272	0.218	2425	1.5”
12.	1 x 0.93” G5 TiB2 6 coat 1 x 0.125” G5	5.02272	0.218	2466	1”
13.	1 x 0.93” G5 TiB2 6 coat 1 x 0.125” G5	5.02272	0.218	2486	1”

D. TEST SERIES 4

The final test series focused on the ceramic ball and fiber backed systems described in III.B.4-5. As previously mentioned, the ceramic balls of diameters 1/8,” 5/32,” 3/16,” and 7/32,” were suspended in a high-tensile strength polyurea foam on the front surface of Ti6Al4V plates. The plate thickness was chosen for each ball diameter so that the overall areal density would not exceed 5 lbs/in^2. The results of these ballistics tests are tabulated in Table 15.

For targets prepared using the fiber backed approach, the number of UHMWPE sheets was chosen to meet the maximum 8 millimeter (0.315 in) overall thickness for plates of thickness 0.032 in, 0.093 in, 0.125 in, and 0.155 in. None of these targets (shown in Table 16) came close to exceeding the areal density constraint. In this table, “CP” indicates that the bullet penetrated the entire system. PC blocks were not utilized for these targets.

Table 15. Test series 4: Ceramic balls

Target #	Target Description	Areal Density (lb/ft2)	Thickness (in)	Velocity (ft/s)	Penetration Depth (in)
61.	1/8 Al2O3 0.155” G5	5.160161568	0.28	2458	1”
62.	5/32 SiC 0.125” G5	4.701631047	0.28125	2446	1”
63.	3/16 Al2O3 0.093” G5	4.526162352	0.2805	2432	1”
64.	7/32 Al2O3 0.093” G5	4.923402744	2.426333	2476	1”

Table 16. Test series 4: Fiber-backed system

Target #	Target Description	Areal Density (lb/ft2)	Thickness (in)	Velocity (ft/s)	Penetration Depth (in)
65	0.032” G5 26 ply UHMWPE	0.747144482	0.315	2395	CP
67	0.0935” G5 21 ply UHMWPE	2.150888459	0.315	2435	CP
69	0.125” G5 18 ply UHMWPE	2.887278743	0.315	2484	CP
71	0.155” G5 15 ply UHMWPE	3.577644633	0.315	2448	CP

E. HARDNESS MEASUREMENTS

Table 17 was produced by performing Brinell, Rockwell C, and Vickers (Micro) hardness tests on 8 different samples. For each test, multiple measurements were taken and then averaged (averaged values shown in dark cells). Table 18 are the results of the nanoindentation process.

Table 17. Hardness test measurements

	Plain	TiN	AlTiN		TiB2			
			Single	Double	Single	Double	4 coats	6 coats
HBW	337	345	297	337	331	317	325	507
	335	341	350	341	337	348	345	354
	329	345	331	339	339	333	363	378
	319	341	354	333	321	345	341	335
	313	333	323	339	317	309	383	350
HBW avg	326.6	341	331	337.8	329	330.4	351.4	384.8
HRC	35.3	36	39	39.5	39	38	39	39.5
	36	36	39	39.5	40	38.5	39	39.5
	36	35	39	39	39.5	39	40	40
	37	35.5	38	39	40	39	39	39
		36.5	39	39	39.5	39	40	39
HRC avg	36.075	35.8	38.8	39.2	39.6	38.7	39.4	39.4
HV (9.8N)	301.7	891.8	585	455.6	527.4	741.8	665.2	1284.2
	358.7	712.9	459.9	545.6	545.6	744.8	808.2	839.5
	339.6	699.2	553.2	551.3	572.8	628.9	688.4	801.5
	357.7	670.2	479.3	477.8	553.2	672.8	652.8	853.9
HV avg	339.425	743.525	519.35	507.575	549.75	697.075	703.65	944.775
HV (4.9N)	348.3	445.9	883.2	638.8	579.5	851.4	774.5	662.9
	376.9	594.3	638.8	485.5	510.9	958.6	474.6	579.5
	349.6	645.5	503.8	548.9	612.8	695.9	752.6	821.3
	356.5	603.4	711.5	487.8	565.3	905.5	802.1	856.6
HV avg	357.825	572.275	684.325	540.25	567.125	852.85	700.95	730.075
HV total avg	348.625	657.9	601.8375	523.9125	558.4375	774.9625	702.3	837.425

Table 18. Nanoindentation hardness (GPa)

	AlTiN		Ti6Al4V		TiB2		TiN	
Test	Avg Modulus	Avg Hardness	Avg Modulus	Avg Hardness	Avg Modulus	Avg Hardness	Avg Modulus	Avg Hardness
1	102.2	3.06	123.8	4.89	315.1	25.83	232.5	10.17
2	69.4	2.24	83	2.7	241.8	17.03	****	****
3	103.5	4.97	114.5	4.5	311.3	27.62	163.7	7.87
Mean	91.7	3.42	107.1	4.03	289.4	23.5	198.1	9.02
Std. Dev.	19.4	1.4	21.4	1.17	41.3	5.67	48.6	1.63
% COV	21.11	41	19.99	28.94	14.26	24.13	24.55	18.07

F. COMPUTATIONAL MODELS

After running a CTH program, an output file is generated that details information (position, velocity, density, pressure, temperature, etc.) of predefined tracers for each time step of a simulation. Four tracers were placed in the following locations (Figure 18):

1. Along the y-axis at the back face of the target
2. Along the y-axis at the middle of the target (Ti6Al4V plate interface for binary targets)
3. Along the y-axis at the tip of the bullet (in contact with the target face)
4. At the front right edge of the core’s face
5. Along the y-axis at the widest part of the bullet’s steel core

Tracer 3 was used to indicate the position of the bullet as it relates to penetration depth into the target. Tracer 5 was used for velocity values because it represents the approximately the center of mass of the bullet after deformation occurs. The x-position of Tracer 4 was used to gauge changes in the radius of the core during impact.

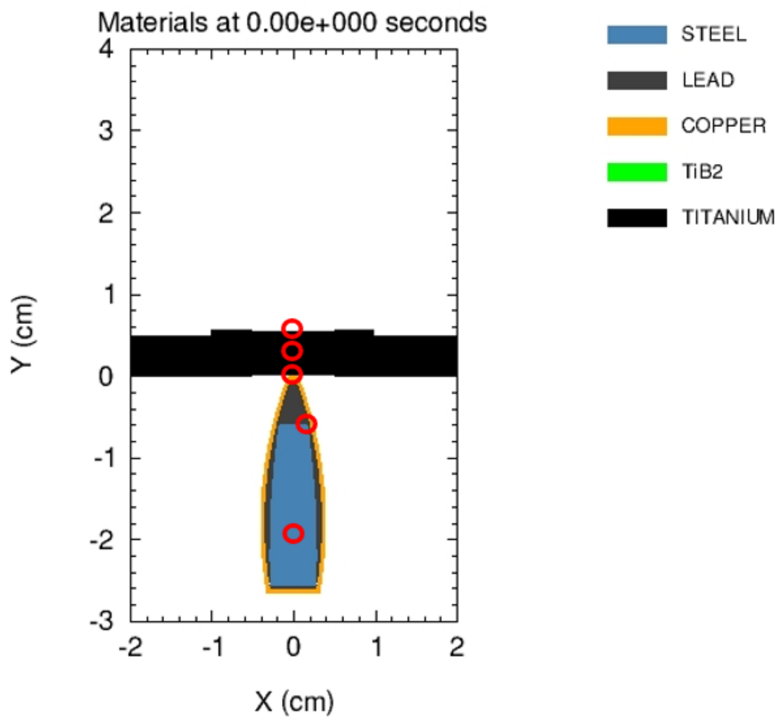

Figure 18. Tracer placement for CTH simulations

1. Laminate Studies

The following figures are visual representations of the simulation results.

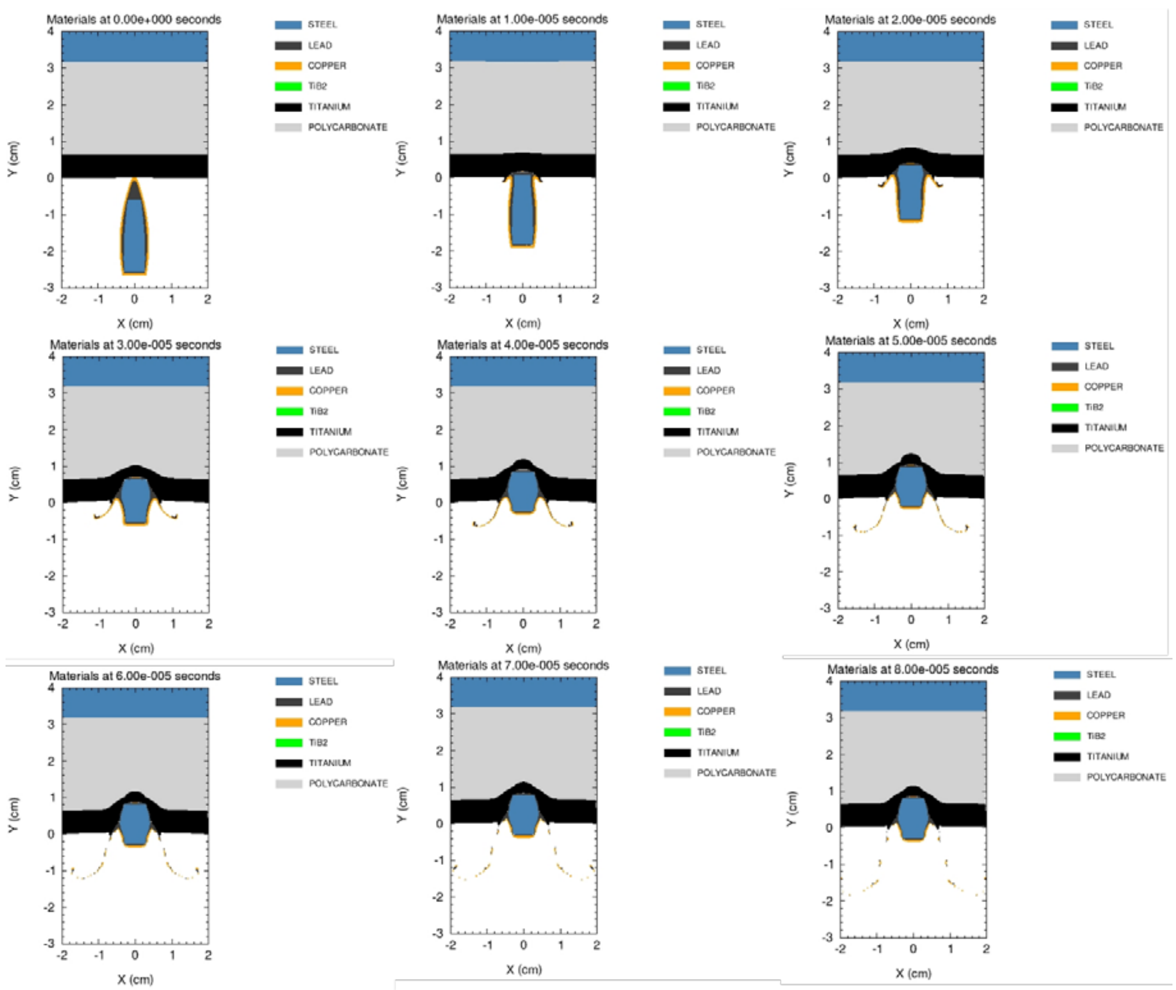

Figure 19. Laminate studies: Material positions during penetration (binary)

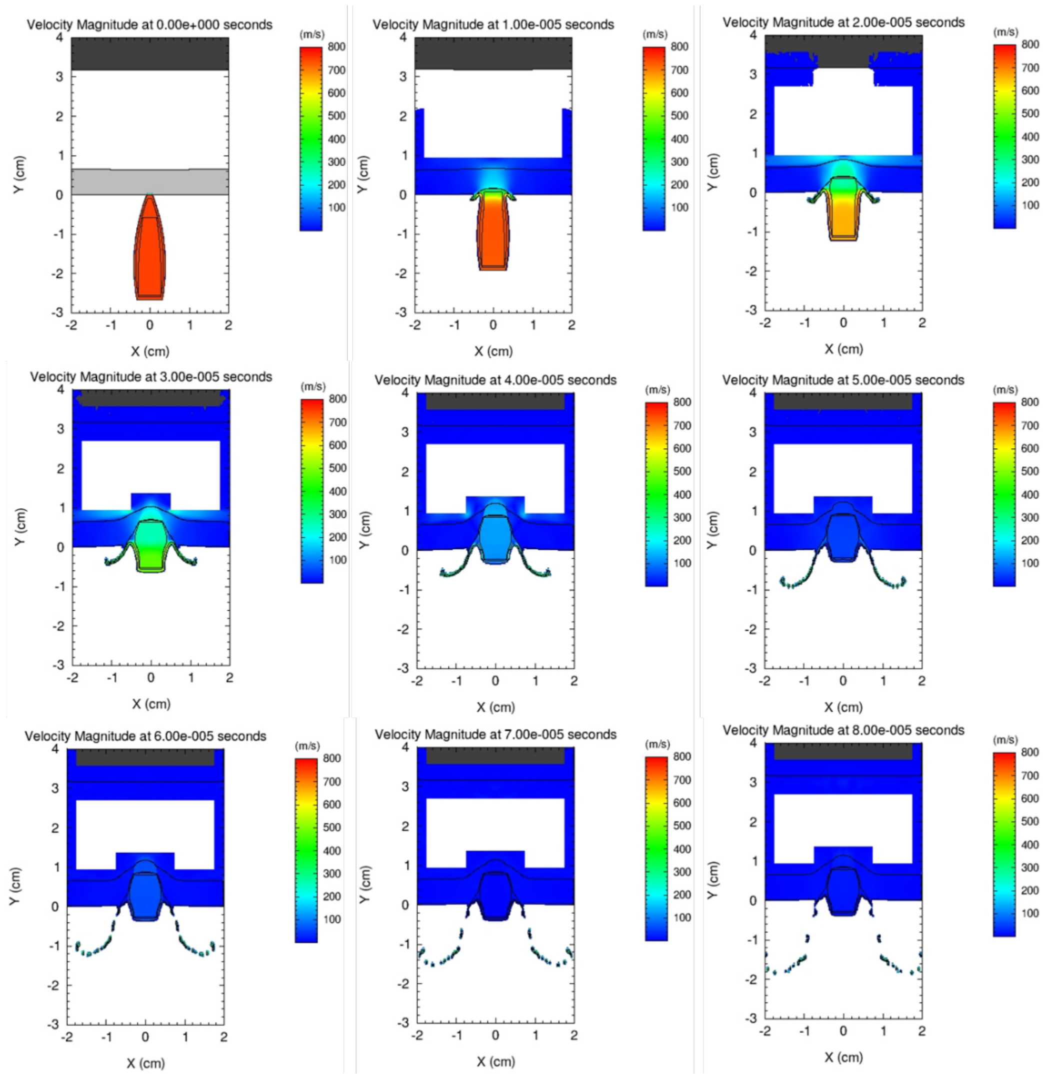

Figure 20. Laminate studies: Velocity of materials during penetration (binary)

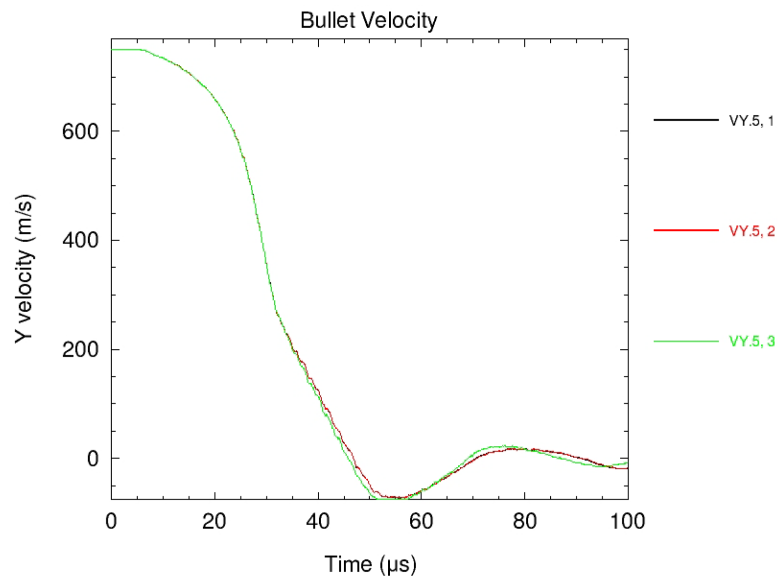

Y-velocity of tracer 5 (VY.5) for monolithic (1), binary (2), and laminate (3) targets.

Figure 21. Laminate studies: Bullet velocity over time

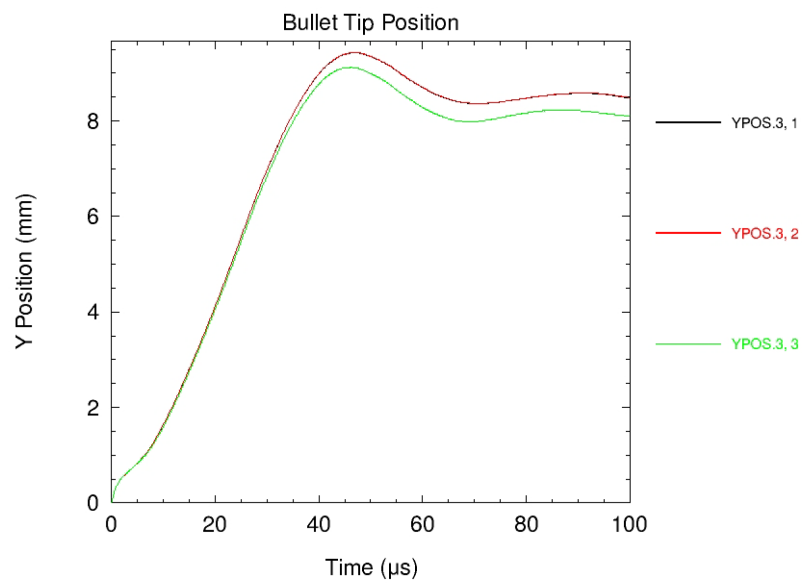

Y-position of tracer 5 (YPOS.3) for monolithic (1), binary (2), and laminate (3) targets.

Figure 22. Laminate studies: Bullet tip position over time

2. Coating Studies

The following figures are visual representations of the simulation results.

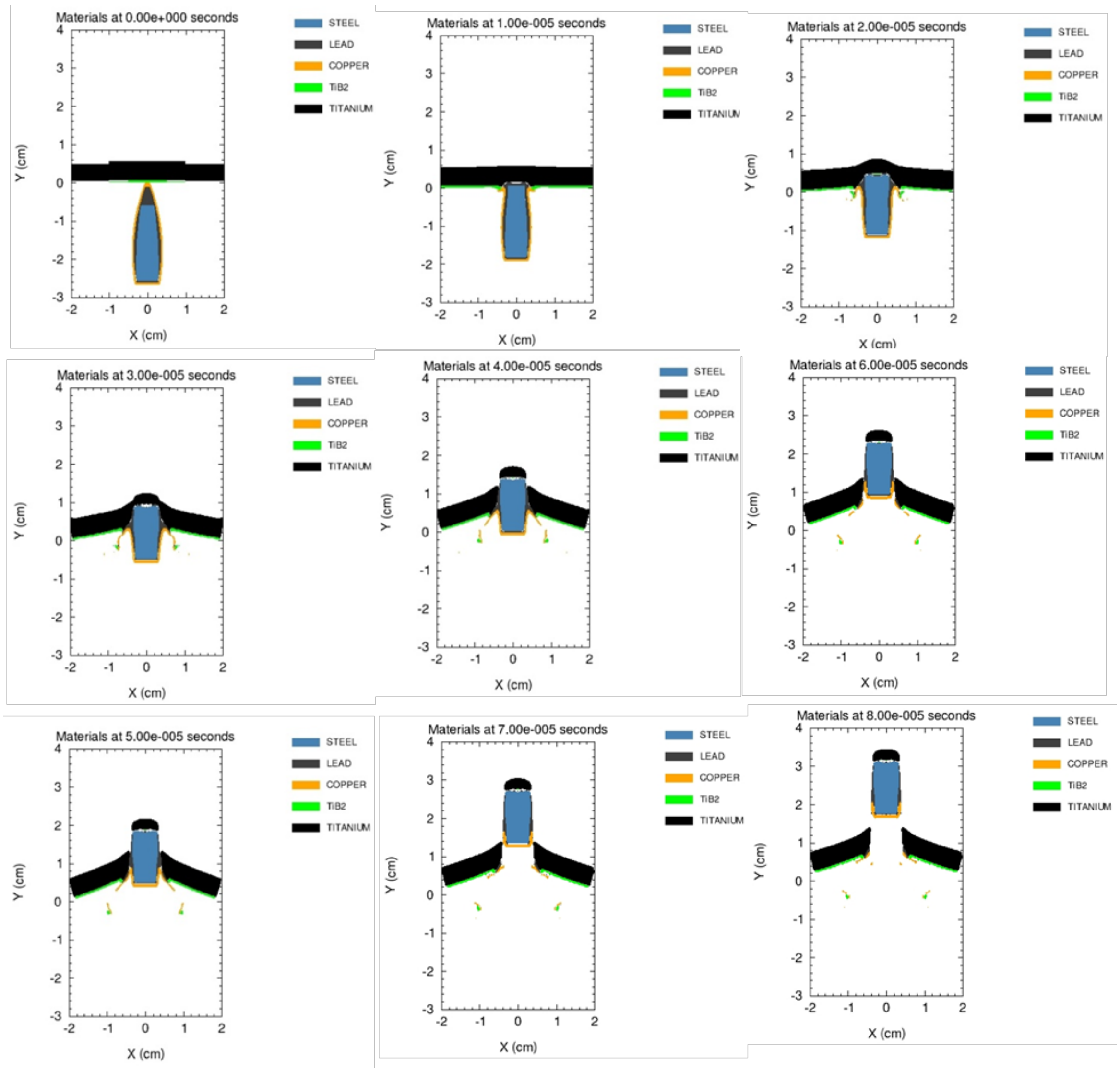

Figure 23. Coating studies: Material positions during penetration (0.5 mm coating)

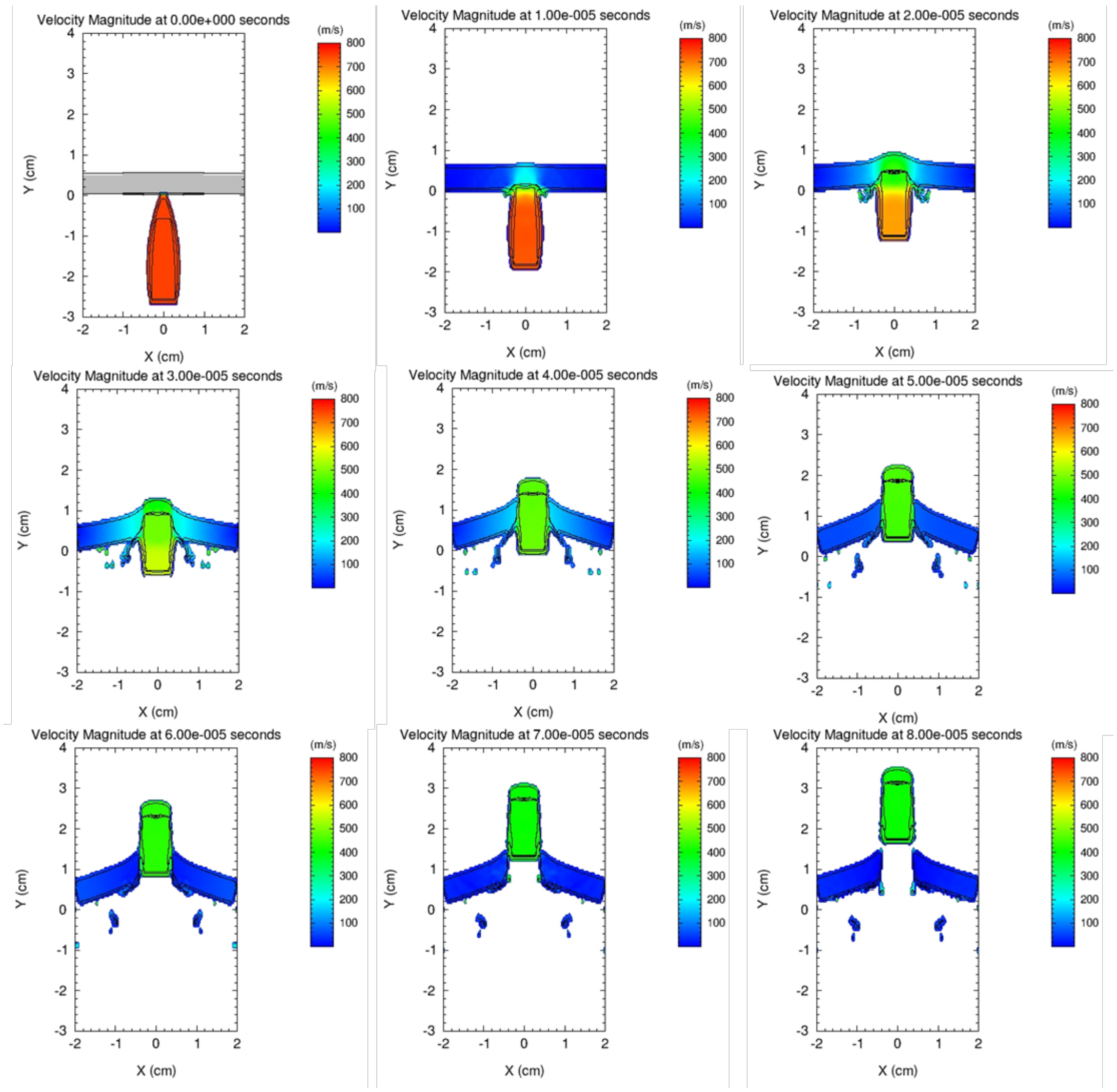

Figure 24. Coating studies: Velocity of materials during penetration (0.5 mm coating)

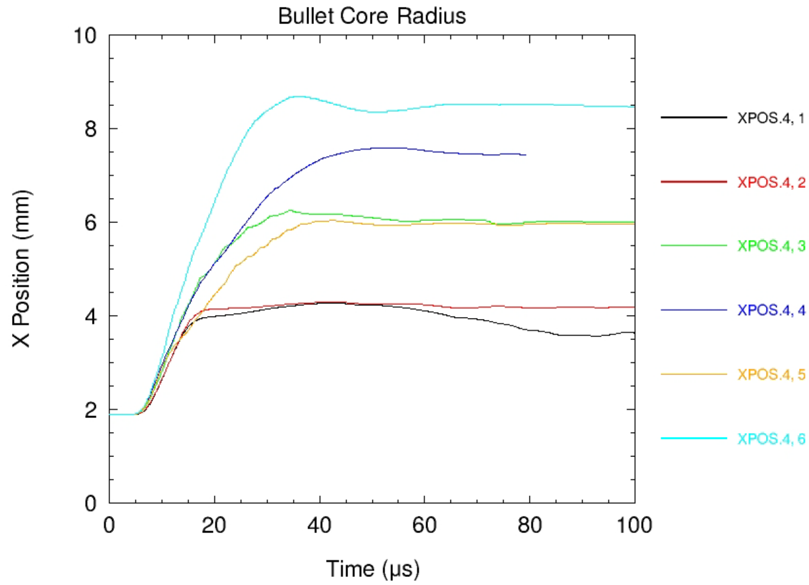

X-position of tracer 4 (XPOS.4) for targets with coating thickness 0.00 mm (1), 0.20 mm (2), 0.40 mm (3), 0.60 mm (4), 0.80 mm (5), and 1.00 mm (6) recorded every 1.00E-7 seconds.

Figure 25. Coating studies: Bullet core radius over time for even-numbered tests

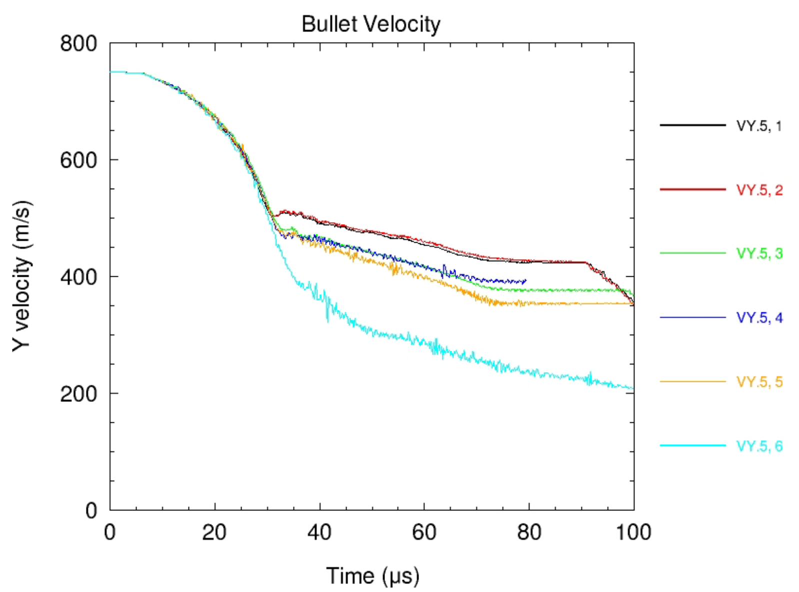

Y-velocity of tracer 5 (VY.5) for targets with coating thickness 0.00 mm (1), 0.20 mm (2), 0.40 mm (3), 0.60 mm (4), 0.80 mm (5), and 1.00 mm (6) recorded every 1.00E-7 seconds.

Figure 26. Coating studies: Bullet velocity over time for even-numbered tests

V. DATA ANALYSIS

A. KEY FINDINGS FROM BALLISTIC TESTS

1. Laminar Systems

a. Laminates perform better than monolithic

Several tests demonstrated that targets with multiple layers (laminate) performed better than monolithic targets of the same thickness. One example is shown in Table 18, in which two targets, one composed of ten thin Ti6Al4V plates and the other composed of a single thick Ti6Al4V plate, are compared. The laminate system successfully stopped the bullet, while the monolithic system allowed 1 inch of penetration into the polycarbonate backing, despite all other variables being the same. This phenomenon suggests that the absence of shear stresses between laminar plates creates better conditions for kinetic energy absorption. A theory is that as the projectile propagates through the laminates an amplification of the front face of the projectile occurs.

Table 19. Laminate-monolithic comparison

Target #	Target Description	Total Thickness (in)	Penetration depth (in)
87	10 G5 plates (0.032" ea)	0.3245	0
118	1 G5 plate	0.3215	1

b. Titanium grade 2 is ineffective

Virtually every target which contained titanium G2 performed poorly as compared to homogeneous Ti6Al4V targets of approximately the same thickness and areal density. This is demonstrated in Table 19, in which a clear trend between three otherwise identical targets can be observed. Data such as these suggest titanium G2 is not a viable material for armor systems.

Table 20. Titanium grade 2 and grade 5 (Ti6Al4V) comparison

Target #	Target Description	Total Thickness (in)	Penetration depth (in)
85	10 G2 plates (0.032" ea)	0.320	> 2
87	10 G5 plates (0.032" ea)	0.325	0
94	10 Alternating plates (0.032" ea)	0.318	1.45

c. Binary systems are reliably effective

Targets comprising only two Ti6Al4V plates are markedly more effective at preventing penetration than monolithic targets of the same thickness. Table 20, along with the data in Table 13 from Test Series 3, shows this clearly. Two plates of thickness 0.125 inches are enough to stop a bullet fired from an AK-47 regardless of the PC backing thickness. This suggests that if the areal density can be slightly reduced (see design constraints I.B.1), a binary armor system is a possible solution for this problem.

Table 21. Binary-monolithic comparison

Target #	Target Description	Total Thickness (in)	Penetration depth (in)
113	1 G5 plate	0.253	> 2
127	2 G5 plates (0.125" ea)	0.251	0

2. Ceramic Plate Systems

a. Thicker ceramic front face plates perform better

During Test Series 1, twenty-nine targets with ceramic front faces were shot (Table 10). The data showed that a ceramic layer is extremely effective at improving the performance of the target. Further, the effectiveness of the ceramic plate is highly dependent on its thickness. This is an unsurprising result, as thick ceramic plates are already used in modern armor systems (see I.A). Table 21 is one example of this trend. Both targets include 0.09-inch monolithic Ti6Al4V plates which, alone, would certainly be incapable of stopping a bullet. A difference of 0.06 inches in ceramic thickness was observed to turn complete penetration of the target/backing assembly into complete stoppage, despite Boron Nitride (BN) and Silicon Carbide (SiC) having similar hardness ratings (BN is rated 9.5 and SiC is rated 9 on the Mohs scale) [11].

Table 22. Ceramic plate thickness comparison

Target #	Target Description	Total Thickness (in)	Penetration depth (in)
71	1 G5 plate (0.09"), 0.125" BN	0.224	> 2
72	1 G5 plate (0.09"), 0.190" SiC	0.283	0

b. Ti6Al4V is the best substrate

Targets comprising ceramic plates of the same material and thickness were shown to be more effective if backed by Ti6Al4V plates than if backed by similar titanium G2 plates. This result concurs with the previous observation (see V.A.b.) that G2 is a generally less suitable material for armor systems. Table 22 shows one example of this occurrence.

Table 23. Titanium grade 5 (Ti6Al4V) and grade 2 ceramic plate substrate comparison

Target #	Target Description	Total Thickness (in)	Penetration depth (in)
76	2 G5 plates, 0.0625" Al2O3	0.206	0.574
74	2 G2 plate, 0.0625" Al2O3	0.208	> 2

3. Surface Coatings

a. Multi-layer coatings are generally more effective

Ceramic coatings did improve ballistic performance of Ti6Al4V targets. Further, thicker coatings were shown to be more effective at improving penetration resistance than thinner coatings. A single layer of TiB_2 is approximately 2 microns thick, whereas single layers of the other surface coatings were about twice that. From test series 2, Table 23 shows this trend for single and double coats of TiB_2 and AlTiN. However, this correlation was weak and did not hold true during test series 3 when 4-layer and 6-layer coats of TiB_2 were observed to perform similarly (Table 24) and to allow deeper penetration than the double coat (Table 23, target 7).

Table 24. Single and double coating comparison

Target #	Target Description	Thickness (in)	Penetration Depth (in)
2.	0.093” G5 TiB2 SC 0.125” G5	0.218	1”
4.	0.093” G5 AlTiN SC 0.125” G5	0.218	1”
7.	0.093” G5 TiB2 DC 0.125” G5	0.218	0.5”
10.	0.093” G5 AlTiN DC 0.125” G5	0.218	0.5”

Table 25. 4-layer coat and 6-layer coat comparison

Target #	Target Description	Thickness (in)	Penetration Depth (in)
10.	1 x 0.93” G5 TiB2 4 coat 1 x 0.125” G5	0.218	1”
12.	1 x 0.93” G5 TiB2 6 coat 1 x 0.125” G5	0.218	1”

b. TiB_2 is the most effective coating

From the data, it can be inferred that TiB_2 is the most effective coating, since it performed just as well as AlTiN despite being half as thick. TiN, which allowed 2” of penetration into the PC, was shown to be the least effective. These results could be predicted from the nominal hardness values of each ceramic (Tables 2–4).

4. Ceramic Balls and Fiber-Backed Systems

The ceramic ball and fiber backed approaches were shown to be ineffective. No target during Test Series 4 was successful at preventing penetration. It is believed that the diameters of the incorporated spheres were not large enough to enable blunting/blunting of the incident threat.

Presumably, to make an effective titanium/UHMWPE armor, the front Ti6Al4V layer would need to provide a harder front face to enable further blunting of the incident projectile and ultimately reducing the projectile pressure on the UHMWPE textile backing system.

B. KEY FINDINGS FROM HARDNESS MEASUREMENTS

1. Indentation Depth Must Be Considered

Shown in Table 26, differences in the Brinell and Rockwell hardness ratings of the ceramic coatings do not seem to be significant. Plain Ti6Al4V was shown to be 36 HRC while Ti6Al4V with 6 coatings of TiB2 were found to be only 39 HRC. This is likely because the indenters pierced through the very thin (~12 μm) layers and measured the hardness of the titanium substrate instead. The Vickers microhardness, on the other hand, did vary in the expected manner with coated samples being over twice as hard as uncoated samples (Figure 27). Microhardness tests typically resulted in indentations on the order of tenths of micrometers (hundreds of nanometers) in depth. While this is certainly enough to penetrate the ceramic coatings, the improved precision does result in a noticeable difference in measurements. For all of these cases, the resulting hardness values are likely a combination of both ceramic and titanium material properties as the indenter penetrated through the coating layers.

Table 26. Hardness measurement comparison

	Plain	TiN	AlTiN		TiB2			
			Single	Double	Single	Double	4 coats	6 coats
HBW avg	326.6	341	331	337.8	329	330.4	351.4	384.8
HRC avg	36.08	35.8	38.8	39.2	39.6	38.7	39.4	39.4
HV avg	348.6	657.9	601.8	523.9	558.4	775.0	702.3	837.4

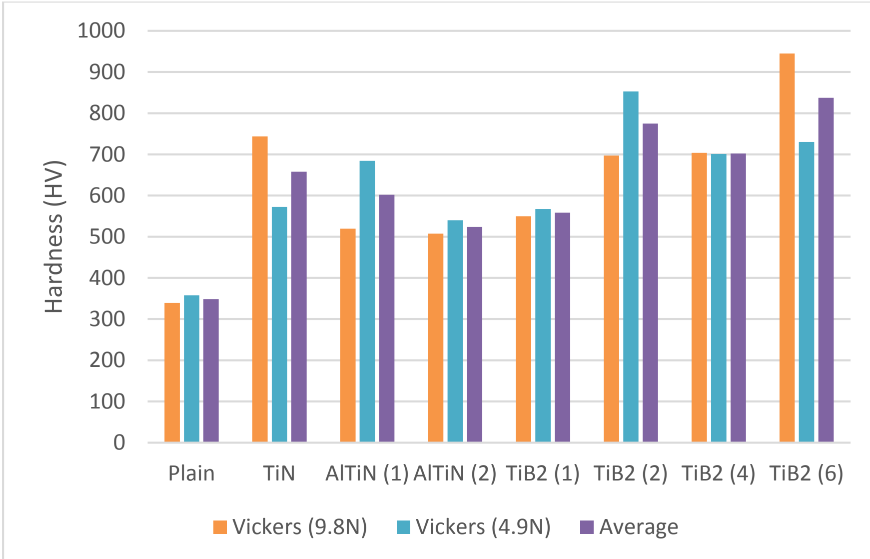

Figure 27. Vickers hardness side-by-side comparison

2. Lower Loads Allow More Variation in Vickers Measurements

As previously discussed, Vickers measurements are made with known applied loads. Theoretically, the hardness value obtained would be the same for a given material regardless of load. However, due to the nature of Vickers micro-indentation, which requires the experimenter to visually inspect the indent under a microscope, there is variation in this method. If the sample surface is not polished, or if the load is too small to make a well-defined impression on the material, it can be difficult to see the edges of the indent, resulting in measurement error. This effect is shown in Table 27, in which the standard deviation of each data set is recorded. The average standard deviation for microhardness tests using a load of 9.8N is 65.85HV, while the average standard deviation for 4.9N tests is 83.31HV. This result implies that high loads allow for more accurate measurements but they cause a further penetration depth into the sample.

Table 27. Deviation in Vickers measurements (9.8N and 4.9N)

	Plain	TiN	AlTiN		TiB2			
			Single	Double	Single	Double	4 Coat	6 Coat
HV (9.8N) Std Dev	23.07	86.98	51.46	41.67	16.28	48.77	61.70	196.9
HV (4.9N) Std Dev	11.45	75.48	136.9	62.32	36.76	98.22	131.86	113.5

3. TiB2 Is the Hardest Coating

According to Kyocera, the nominal hardness of the TiB_2 coating is 4000HV. This value was not corroborated by any of the tests conducted. The nanoindentation hardness was found to be only 23.5 GPa, which is equivalent to 2396HV. However, this result is much higher than any of the others, suggesting that TiB_2 is in fact harder than the other coating materials. The lower value is believed to be due to the thin coating layers and the required polishing which further removes from the coating thickness.

4. Great Care Must Be Taken When Polishing Nanoindentation Samples

Shown in Table 28, the Ti6Al4V sample coated with AlTiN was just as soft as the one without. This is likely due to the coating being abraded off during the preparation process. Samples for future tests should be polished using only very fine (>1200 grit) abrasive.

Table 28. Nanoindentation hardness (GPa and HV) comparison

	Plain Ti6Al4V	TiN	AlTiN	TiB2
Nano Hardness (GPa)	4.03	9.02	3.42	23.5
Nano Hardness (HV)	410.9	919.8	348.7	2396
Nominal	350	2200	3300	4000

C. KEY FINDINGS FROM CTH MODELS

1. Laminate Studies

a. CTH does not accurately reflect ballistics tests

In the ballistics tests analyzed above, 0.25” monolithic targets proved incapable of stopping a 7.62x39 mm ball round traveling at muzzle velocity while a binary target of the same thickness was reliably effective (see V.A.1.b.). In the CTH simulations, however, the performances of monolithic and binary targets were virtually identical. The 8-layer laminar target was slightly more effective, limiting the penetration distance to 8.0 mm into the target (approximately 0.5 mm shallower than monolithic and binary targets). In ballistics tests, the corresponding targets were not this successful (Table 8). This result suggests that CTH simulations alone are not sufficient for designing armor concepts.

b. All targets prevented penetration

Discussed above, the three tested target configurations were all successful in stopping the bullet. With this information, along with ballistics test data, it can be concluded that a binary laminate equaling 0.25” thickness of Ti6Al4V is sufficient for absorbing the kinetic energy of an AK-47 round. Unfortunately, this thickness exceeds the areal density constraint by 0.75 lbs/ft^2.

2. Coating Studies

a. No target prevented penetration

It is worth noting that, for the simulated configuration, none of the targets with TiB_2 coating thickness of 1.00 mm or less successfully prevented penetration. This result implies that a successful design that conforms to the constraints outlined in I.B.1. would need a very thick (> 1.00 mm) ceramic coating. To achieve this thickness with TiB_2, at least five-hundred coats would need to be applied to the Ti6Al4V face.

However, this result should not be directly compared to those of ballistics tests because the conditions were not set up in the same way. No PC backing was present which allowed more deformation of the Ti6Al4V plates than would likely be seen in a real scenario. Therefore, data should be considered only relative to similar CTH simulations and acted on qualitatively.

b. Impact area amplification is a function of coating thickness

It can be easily seen that increased coating thicknesses resulted in greater core radii after impact. In the uncoated simulation, the radius of the core’s front face increased from 1.9 cm to a maximum of approximately 4.0 cm. This means Ti6Al4V alone is capable of amplifying impact area of the bullet by over 300%. When a 0.40 mm layer of was TiB_2 was added, this number quadrupled to over 1200%. Dilation of the bullet’s core can thus be attributed to the harder impact surface provided by ceramic. As discussed in II.C., impact area amplification results in decreased impact pressure and therefore greater penetration resistance. Figure 28 shows a weak trend in maximum core radius with respect to core radius. The improvement becomes apparent after 0.30 mm.

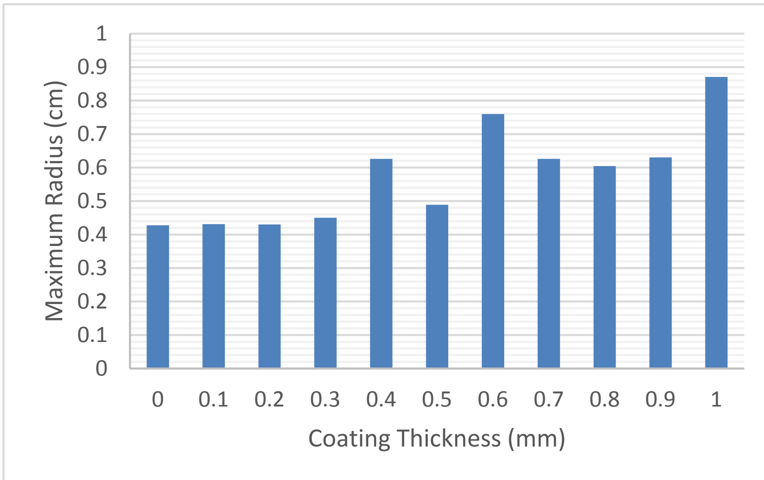

Figure 28. Maximum core radius for TiB_2 coating thicknesses (0.0–1.0 mm)

c. Exit velocity is a function of coating thickness

There is a loose correlation between exit velocity (the velocity of the bullet after complete penetration has occurred) and coating thickness. When passing through the plain target, the projectile loses over half of its initial kinetic energy. When passing through targets coated with at least 0.30 mm of TiB_2, this effect is even greater. This result is useful because it gives us an idea of how effective the armor system would be at absorbing impact energy.

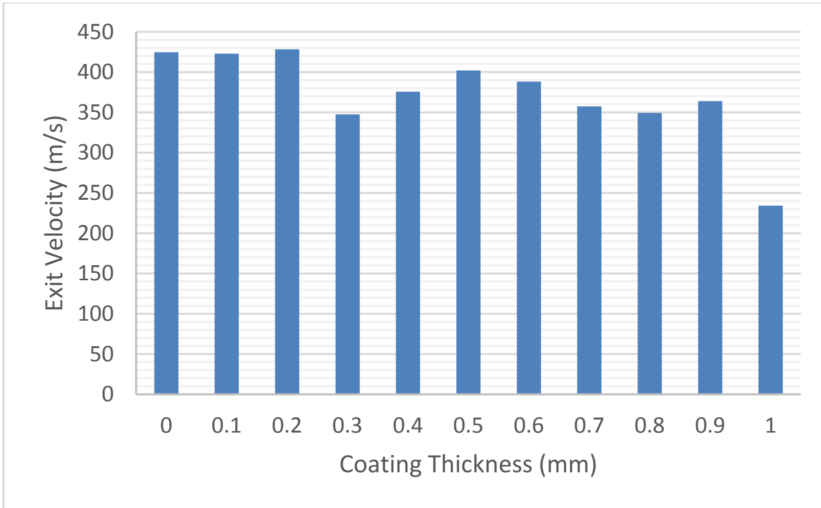

Figure 29. Exit velocity for TiB_2 coating thicknesses (0.0–1.0 mm)

VI. CONCLUSION

A. SUMMARY

In an effort to produce a lightweight, low-profile body armor, several approaches were explored and tested with varying success. Titanium was chosen as an armor material because of its relatively low density (4.5 g/cm^3), high strength (up to 895 MPa for Ti6Al4V) and its superplastic formation behavior.

Ballistic tests demonstrated that performance of a titanium armor system could be improved through the employment of a layered, or laminar, system which is understood to reduce shear stresses in the material during penetration. Test samples prepared using two 0.125" Ti6Al4V plates were consistently effective at stopping 7.52x39mm ball rounds traveling at or near AK-47 muzzle velocity (747 m/s). This result was validated by computer simulations. Adding a hard ceramic front face to any titanium system was also shown to significantly improve ballistic performance. Titanium grade 2 was found to be ineffective in virtually any configuration, even when paired with Ti6Al4V in heterogeneous laminar targets. Monolithic G2 targets demonstrated little penetration resistance even at thickness of up to 0.313." Monolithic Ti6Al4V targets performed slightly better but penetration depth was inconsistent.

Computer models suggest that a binary Ti6Al4V system with a very thick (>1 mm) front coating of TiB_2 is a solution to the proposed problem (Figure 30). While simulation results indicate a residual projectile velocity of approximately 230 m/s, it is reasonable to expect ballistic experimentation to demonstrate the improved penetration resistance of binary systems.

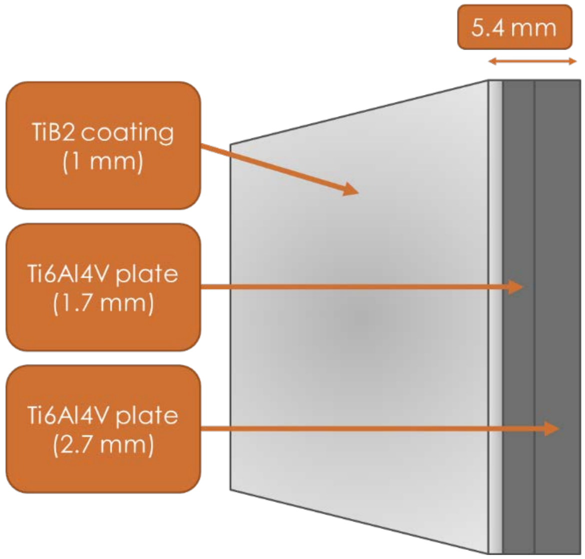

Figure 30. Potential solution

B. FUTURE WORK: SUPERPLASTIC FORMATION

1. Theory

As discussed in I.F., Ti6Al4V exhibits superplastic behavior, allowing it to be formed to over 1000% elongation without undergoing harmful material property changes. If such an armor system were to be fabricated, this property could be leveraged to simplify the process. That is, the titanium plates could be superplastically formed into a torso-shaped die or mold and coated with a thick layer of ceramic. Future work should explore this possibility before a dual-hardness laminar Ti6Al4V body armor concept is employed.

2. Methodology

Ti6Al4V begins to behave superplastically between 840°C and 870° [4]. Sheet Ti6Al4V would be placed on an airtight steel die and heated in a furnace to this temperature. Next, an inert gas such as Argon would be pumped in at an appropriate pressure, uniformly pressing the now malleable sheet into the die. This must be done slowly, or hardening will occur preventing any further superplastic strain. After cooling, the gas would be released and the formed Ti6Al4V would be extracted. It is possible this process could be done with multiple plates at a time, resulting in a homogeneous laminar system held together by its own geometry. Figure 31 is a basic diagram of this process.

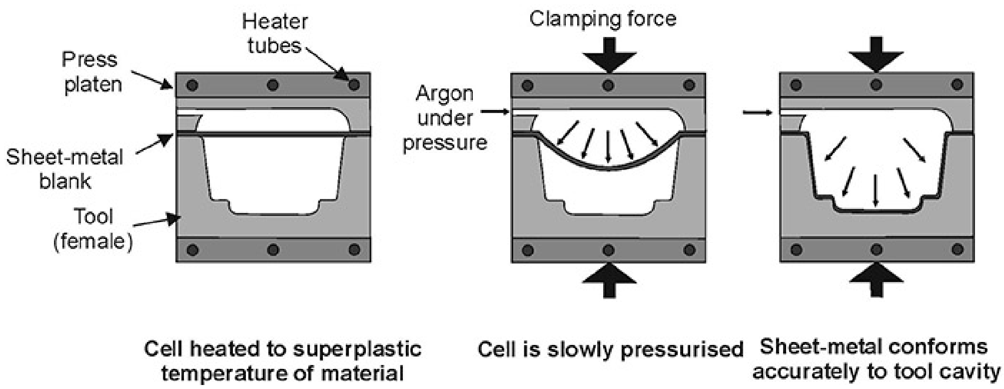

Licensed by Creative Commons and obtained through Microsoft Office image search

Figure 31. Schematic of superplastic forming

3. Proof of Concept

In anticipation of this future work, a proof-of-concept die was designed and machined (shown in Figure 32). Fabricated from steel, the cylindrical die is 5” in diameter with a 3” diameter hemispherical cavity. 1/8” deep groves provide a place for a rubber gasket to sit and create an airtight seal around the chamber. The lid or platen is designed to be secured with six 1/4” fasteners and features a tapped hole for connecting an air pump. The Ti6Al4V plates, which are 5” diameter circles with six bolt holes would be placed between the die and the platen.

Figure 32. Proof-of-concept die for superplastic formation studies

THIS PAGE INTENTIONALLY LEFT BLANK

LIST OF REFERENCES

[1] A. Tate, "A theory for the deceleration of long rods after impact," *Journal of Mechanics and Physical Solids*, vol. 15, no. 6, pp. 387–399, 1967.

[2] R. Perkins and E. Rennhack, "Processing and ballistic evaluation of dual-hardness titanium armor," National Technical Information Service, Springfield, VA, USA, AD-777 809, 1974.

[3] A. Zhecheva, W. Sha, S. Malinov and A. Long, "Enhancing the microstructure and properties of titanium alloys through nitriding and other surface engineering methods," *Surface & Coatings Technology*, vol. 200, no. 7, pp. 2192–2207, 2005.

[4] J. D. Beal, R. Boyer, D. Sanders and T. B. Company, "Forming of titanium and titanium alloys," *ASM Handbook*, vol. 14B, Metalworking: Sheet Forming, pp. 656–669, 2006.

[5] C. Roland and R. Gamache, "Measuring the blast and ballistic performance of armor," Naval Research Laboratory, Washington, DC, USA, 2015.

[6] B. Dyatkin and R. Gamache, "Ballistic performance of front-facing fluoropolymer-coated armor composites," *International Journal of Impact Engineering*, vol. 114, pp. 63–68, 2018.

[7] Kyocera Hardcoating Technologies Ltd. Accessed May 1, 2018. [Online]. Available: http://www.kyocera-hardcoating.com/index.html

[8] KLA-Tencor Corporation, "Nano Indenter G200 | Nanomechanical Testers," Accessed May 14, 2018. [Online]. Available: https://www.kla-tencor.com/Nanomechanical-Testers/nano-indenter-g200.html

[9] D. Crawford, "CTH capabilities," Sandia National Laboratory. Accessed May 1, 2018. [Online]. Available: http://www.sandia.gov/CTH/Capabilities-leftnav-level1_js.html

[10] D. A. Crawford, A. L. Brundagge, E. N. Harstad, K. Ruggirello, R. G. Schmitt, S. C. Schumacher and J. S. Simmons, "CTH User's Manual and Input Instructions," CTH Development Project - Sandia National Laboratories, Albuquerque, 2013.

[11] G. Samsonov, "Mechanical properties of the elements," in *Handbook of the Phyicochemical Properties of the Elements*, New York, IFI-Plenum, 1968, p. 432.

THIS PAGE INTENTIONALLY LEFT BLANK

INITIAL DISTRIBUTION LIST

1. Defense Technical Information Center
   Ft. Belvoir, Virginia

2. Dudley Knox Library
   Naval Postgraduate School
   Monterey, California